Energy recovery evaluation and temperature field research of underground coal gasification under different oxygen concentrations

Su, Fa-qiang
School of Energy Science and Engineering, Henan Polytechnic University

Zhang, Tao
School of Energy Science and Engineering, Henan Polytechnic University

Wu, Jun-bo
School of Energy Science and Engineering, Henan Polytechnic University

Deng, Qi-chao
School of Energy Science and Engineering, Henan Polytechnic University

他

出版情報：Fuel. 329, pp.125389-, 2022-12-01. Elsevier
バージョン：

Fuel

Energy recovery evaluation and temperature field research of underground coal gasification under different oxygen concentrations

--Manuscript Draft--

Manuscript Number:	JFUE-D-22-04519R1
Article Type:	Research Paper
Keywords:	Underground coal gasification; Stoichiometry; Coal consumption; Gasification efficiency; Sensible heat
Corresponding Author:	Yi-he Yu Henan Polytechnic University CHINA
First Author:	Fa-qiang Su
Order of Authors:	Fa-qiang Su
	Tao Zhang
	Jun-bo Wu
	Qi-chao Deng
	Akihiro Hamanaka
	Yi-he Yu
	Meng-jia Dai
	Xiao-long He
	Jun-nan Yang
Abstract:	In this paper, UCG simulation experiments are carried out on selected coal samples to study the effects of the gasification agent ratio on the product gas composition and calorific value under different oxygen concentrations. Moreover, an energy recovery evaluation method based on stoichiometric theory is established based on the carbon (C) balance in the generated gas content, and the energy recovery rate and coal consumption of the underground gasification process are evaluated. Based on the composition of the produced gas and the thermodynamic law of conservation, an evaluation model of the underground coal gasification temperature field is established. The gasification chamber temperature in each stage is evaluated by calculating the reaction heat and sensible heat. The experimental and research results showed that when the volume fraction of oxygen in a gasification agent was in the range 40 - 70 % and the calorific value of the produced gas increased from 10.48 MJ/m 3 to 12.48 MJ/m 3 . The calorific value of the produced gas increased with an increasing oxygen concentration. Furthermore, the energy recovery rate increased from 69.63% to 83.88%, indicating that the gasification efficiency of the UCG experiment can be significantly improved with an increasing oxygen concentration. The error between the theoretical value of the coal consumption and the actual monitoring value was within 10%, which effectively evaluates the coal consumption in the gasification process. The theoretical calculation temperature was consistent with the experimental monitoring temperature results, and the reaction heat was found to also be linearly correlated with the gasification temperature. Therefore, this method can effectively determine the gasification chamber temperature. These monitoring and evaluation methods are expected to guide the analysis of subsurface field experiments.
Suggested Reviewers:	Tatiana Selivanova selivanova_d@mail.ru Professor Tatiana Selivanova is famous in this field. We knew that he is very severe and fastidious to manuscripts, we hope he will give us more suggestions to improve ours English and quality of the manuscript.
	Peng Pei peng.pei@und.edu We suggest Prof. Peng Pei to be reviewer for our manuscript in that he has deep

	insight into the research on underground coal gasification.
	Prabu Vairakannu v.prabu@iitg.ernet.in Prof. Prabu Vairakannu is an expert on underground coal gasification. We have found that he has published several paper on underground coal gasification as the corresponding author or the first author.
	Marian Wiatowski mwiatowski@gig.eu He did this very well in the related field.
	Greg Perkins g.perkins@unsw.edu.au His recent publications are related to my study, so he will be familiar with and give fair judgment to my manuscript.

Energy recovery evaluation and temperature field research of underground coal gasification under different oxygen concentrations

Fa-qiang Su[a,b], Tao-Zhang[a], Jun-bo Wu[a], Qi-chao Deng[a], Akihiro Hamanaka[c], Yi-he Yu[a,b,*] Meng-jia Dai[a], Xiao-long He[a], Jun-nan Yang[a]

[a] *School of Energy Science and Engineering, Henan Polytechnic University, Jiaozuo, Henan, 454-003, China*

[b] *State Collaborative Innovation Center of Coal Work Safety and Clean-efficiency Utilization, Henan Polytechnic University, Jiaozuo, Henan, 454-003, China*

[c] *Department of Earth Resources Engineering, Kyushu University, 744 Motooka, Nishi-ku, Fukuoka 819-0395, Japan*

* *Correspondence: yyhcmsj@hpu.edu.cn*

Abstract：

In this paper, UCG simulation experiments were carried out on selected coal samples to study the effects of the gasification agent ratio on the product gas composition and calorific value under different oxygen concentrations. Moreover, an energy recovery evaluation method based on stoichiometric theory was established based on the carbon (C) balance in the generated gas content, and the energy recovery rate and coal consumption of the underground gasification process were evaluated. Based on the composition of the produced gas and the thermodynamic law of conservation, an evaluation model of the underground coal gasification temperature field was established. The gasification chamber temperature in each stage was evaluated by calculating the reaction heat and sensible heat. The experimental and

research results showed that when the volume fraction of oxygen in a gasification agent was in the range 40 - 70 % and the calorific value of the produced gas increased from 10.48 MJ/m^3 to 12.48 MJ/m^3. The calorific value of the produced gas increased with an increasing oxygen concentration. Furthermore, the energy recovery rate increased from 69.63% to 83.88%, indicating that the gasification efficiency of the UCG experiment can be significantly improved with an increasing oxygen concentration. The error between the theoretical value of the coal consumption and the actual monitoring value was within 10%, which effectively evaluates the coal consumption in the gasification process. The theoretical calculation temperature was consistent with the experimental monitoring temperature results, and the reaction heat was found to also be linearly correlated with the gasification temperature. Therefore, this method can effectively determine the gasification chamber temperature. These monitoring and evaluation methods are expected to guide the analysis of subsurface field experiments.

Keywords: Underground coal gasification; Stoichiometry; Coal consumption; Gasification efficiency; Sensible heat

1. Introduction

Underground coal gasification is a complex physicochemical change process that involves heat and mass transfer, fluid flow, gas–solid two-phase chemical reactions, and other problems [1-3]. Compared with traditional coal mining methods, underground coal gasification is not only suitable for the mining of deep, steep, and gently inclined coal seams but can also reduce the mining cost and damage to the environment, which is consistent with the national construction of a low-carbon, clean, safe and efficient modern energy system [4,5].

Underground coal gasification is an industrial means to burn coal resources in situ by injecting gasification agents such as O_2, H_2O and CO_2 to obtain combustible gases such as CH_4, H_2 and CO [6,7]. The coal seam steadily burns when heated, and the underground fire area gradually expands, forming a gradient temperature field [8,9]. The chemical reaction process presents different reaction phenomena under different temperature conditions. Therefore, the following three reaction zones are formed in the

gasification channel: the oxidation zone, reduction zone, and dry distillation zone. Figure 1 shows the temperature range of each reaction zone and the main chemical reactions in the underground coal gasification [10,11].

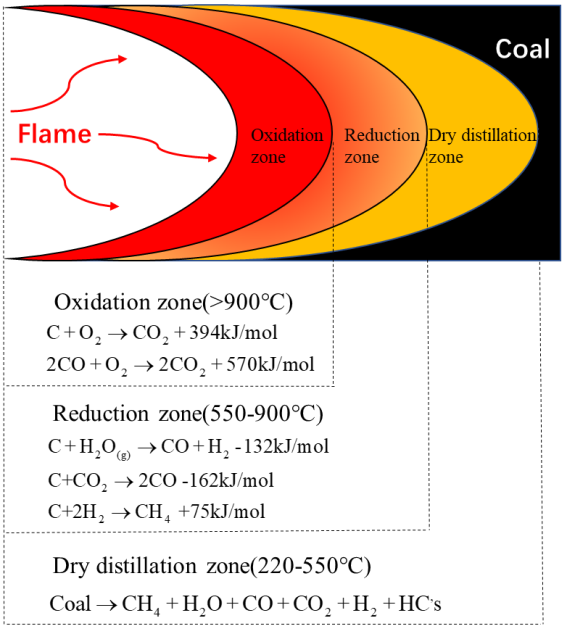

Figure 1. Three zones in the underground coal gasification

The temperature in the oxidation zone usually is higher than 900°C, which is the heat source that promotes the gasification process. The main chemical reactions that produce combustible gases in the UCG process occur in the reduction and dry distillation zones. In terms of the chemical reactions, the three zones are not strictly delineated, but rather the relative strengths and weaknesses of the redox and dry distillation reactions are elaborated [12].

The underground gasification process of coal is complex, and the process flow is unique [13-15]. Currently, scholars in this field have conducted research on the development of gasification cavities, the efficiency of gasification and its influencing factors, and the analysis of the gasification process based on chemical methods. To optimize the efficiency of energy conversion in the process of underground coal gasification, Shuqin Liu and others [16] established an exergy evaluation model of an underground

63 coal gasification system in combination with the first law of thermodynamics and the second law of
64 thermodynamics. E. Andrianopoulos [17] combined chemical process modeling with a UCG-specific
65 underground layout to evaluate the quality of the syngas produced. Renato Zagorščak [18]
66 experimentally investigated the effects of different pressures and gasification agent ratios on the
67 gasification process. Adam Smoliński [19] analyzed and studied the harmful inorganic substances in the
68 wastewater that was produced in the process of underground coal gasification by chemical methods.
69 However, there are relatively few theoretical and experimental studies that is based on the chemometrics
70 theory to evaluate the energy recovery in the whole process of underground coal gasification.
71 Additionally, accurate methods that are generally suitable for evaluating the efficiency of underground
72 coal gasification are lacking.

73 Gasification agents with different oxygen concentrations directly affect the temperature of the
74 gasification area, while the UCG process is a self-heat balance process [20]. The heat generated by
75 combustion is conducive to establishing the ideal temperature field of the underground gasifier and leads
76 to a reduction reaction and decomposition reaction, which finally produces gas [21]. Therefore, in the
77 UCG process, mastering the temperature field distribution law of the UCG extraction field is not only
78 crucial for further research on the development of the combustion void zone and the structure and size
79 parameters of the gasifier, but also provide meaningful guidance for the improvement in gasification
80 technology and the development of combustion control technology [22-24]. The dynamic evolution of
81 the temperature field affects the stability of the underground coal gasification process; thus, many
82 researchers are attentive to the research of the temperature field. By considering the wet coal area and
83 dry distillation area, Massaquoi and Riggs [25] established a one-dimensional mathematical model to
84 predict the combustion process of underground coal gasification. Based on the model test, Lanhe Yang

85 [26] established a two-dimensional linear dynamic mathematical model of the temperature field of the
86 gasification layer, and calculated the parameters by the control volume method. In addition, the
87 calculated values that were obtained by the model are consistent with the measured values. Jianfen Xi
88 and others [27] used Ulanqab lignite to study the dynamic expansion of the underground coal seam
89 temperature field, and concluded that the expansion of the temperature field is mainly affected by the
90 coal seam fissures and gasification agent flow. With the in-depth study of underground coal gasification,
91 the temperature field is developing in the direction of the mechanism, three dimensions and whole
92 process. After years of research and field practice, underground coal gasification technology has achieved
93 remarkable results. Due to the complexity and invisibility of underground coal gasification, attaining
94 long-term stable production and commercial development still needs further research and improvement
95 [28-33].
96 This underground coal gasification experiment adopted a horizontal hole gasification channel. This
97 study combined experimental and theoretical analyses, which is expected to provide a theoretical basis
98 for the field experiment of underground coal gasification. The main objectives of this study are as follow:
99 a) to determine the effect of the different oxygen concentrations on the product gas compositions; b) to
100 determine the effect of the temperature on the product gas compositions; c) to evaluate gasification
101 efficiency using a proposed stoichiometric approach; and d) to estimate gasifier temperature using a
102 proposed heat balance theory.

103 **2.Materials and Methods**

104 **2.1 Experimental apparatus**

105 The experiment was carried out in the Energy Research Laboratory of Henan University of Polytechnic.
106 The experimental system of the UCG model comprises the main gasifier body, gasifying agent injection

system, cooling, purification system, and monitoring system. The experimental setup is shown in Figure 2. The main body of the gasifier was made of a steel container, and the external dimension was 2.0 m (length)×1.0 m (width)×1.0 m (height). External walls of the simulated coal seam were covered with refractory cement to prevent heat release and gas leakage. In the lower part of the gasifier at 40 mm from the bottom of the furnace, a horizontal gasification channel was made of hollow steel spring with an inner diameter of 50 mm to prevent the collapse of the coal layer from blocking the gasification channel during the combustion process. The gasifying agent injection system was composed of an air compressor and oxygen generator to provide enough air and oxygen (Pure oxygen) for the experiment. The cooling and purification system was composed of a cooling box and purification box, which are used to cool and filter out impurities such as tar in the gas. A temperature sensor was arranged in the borehole above the coal seam to monitor the temperature of the gasification area in real time. A sampling pump was set in front of the inlet end of the gas chromatograph; this device can effectively pump the gasified gas to the gas chromatograph under the condition of small flow, which can more accurately analyze the gas composition after gasification. The electronic scale under the gasifier monitored the change in the coal seam weight in real time.

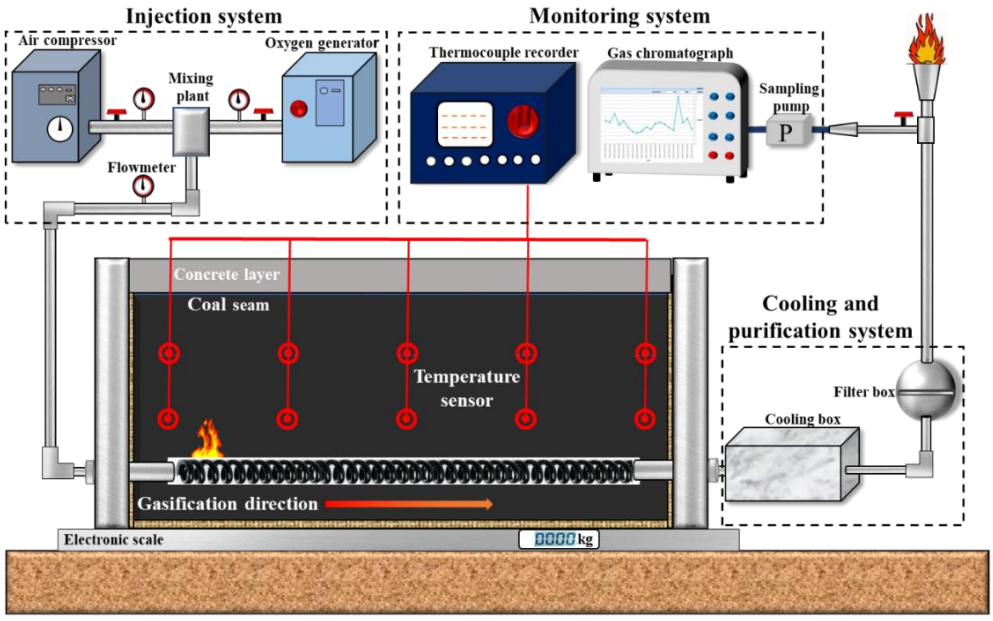

Figure 2. UCG experimental system

2.2 Experimental procedure

2.2.1 Gasification coal sample

In the gasifier, the artificial coal seam was laid layer by layer with coal blocks of length and width of about 100 mm. Additionally, the laying thickness was 400 mm. In the laying process, 100 mm was used as the laying thickness unit 4 times. Each time, the laying plane would be compacted to ensure the structural stability of the artificial coal seam in the gasification process. After the bottom coal seam was laid to 40 mm, the ceramic electric heating ignition plate was embedded. Combustion supporting materials, such as solid alcohol and wood chips, were placed above the ignition disc (Figure 4).

The experimental coal samples were obtained from the Bojianghaizi coal mine in Ordos, Inner Mongolia, China. The results of the proximate analysis and ultimate analysis are shown in Table 1.

Table 1. Proximate and ultimate analysis of coal

No.	Parameter	Value
	Proximate analysis (wt%)	
1	Moisture	3.19
2	Ash	9.2
3	Volatiles	33.06

4	Fixed carbon	54.55
	Ultimate analysis (wt%)	
5	Carbon	79.745
6	Hydrogen	4.42
7	Nitrogen	1.005
8	Oxygen	10.445
9	Sulfur	0.185
10	Calorific value (MJ/kg)	25.74

2.2.2 Gasification agent

Oxygen-enriched air was mainly used as the gasification agent in the experiment. The effects of the oxygen concentration in the gasification agent on the calorific value, temperature, and gasification efficiency were investigated on the premise of other constant test parameters. The injection flow of this gasification experiment is shown in Figure 3. The experiment is carried out in four stages, and the total injection rate of the gasification agent in each stage was constant at 7 m^3/h. The air injection rates of the four stages were 5.3 m^3/h, 4.4 m^3/h, 3.5 m^3/h, and 2.7 m^3/h; the oxygen injection rates were 1.7 m^3/h, 2.6 m^3/h, 3.5 m^3/h, and 4.3 m^3/h; and the oxygen concentrations in the gasification agent were 40%, 50%, 60%, and 70%, respectively.

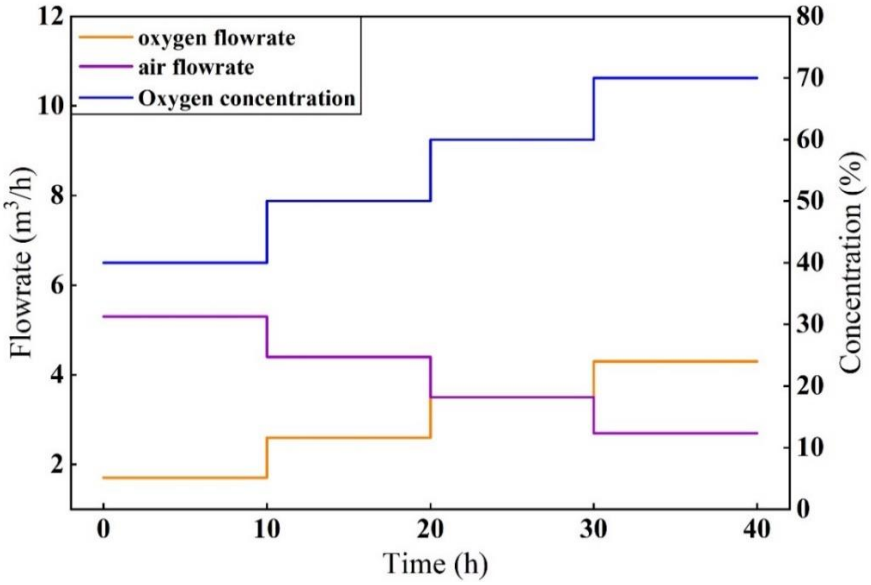

Figure 3. Feed gas flow during the gasification experiments

In the experimental ignition stage, oxygen was introduced into the gasification channel. The igniter was turned on to heat the ignition disk and ignited the combustion supporting materials and nearby coal. The success of the ignition is determined by observing the temperature measured by the thermocouple and the gas composition at the outlet (Figure 4). If the temperature gradually rose to 600℃, the combustible gas components such as H_2, CO and CH_4 continue to rise. The gas generated at the gas production port was successfully ignited, which indicated that the experimental ignition is successful. After the ignition was successful, the gasifying agent was continuously and stably fed in stages according to the preplanned flow, the generated gas was fed into the meteorological chromatograph every 30 minutes to analyze the composition of the produced gas, and the temperature of the gasification chamber and the weight of the gasifier were monitored in real time. At the end of the experiment, N_2 is injected into the gasification area to extinguish the fire.

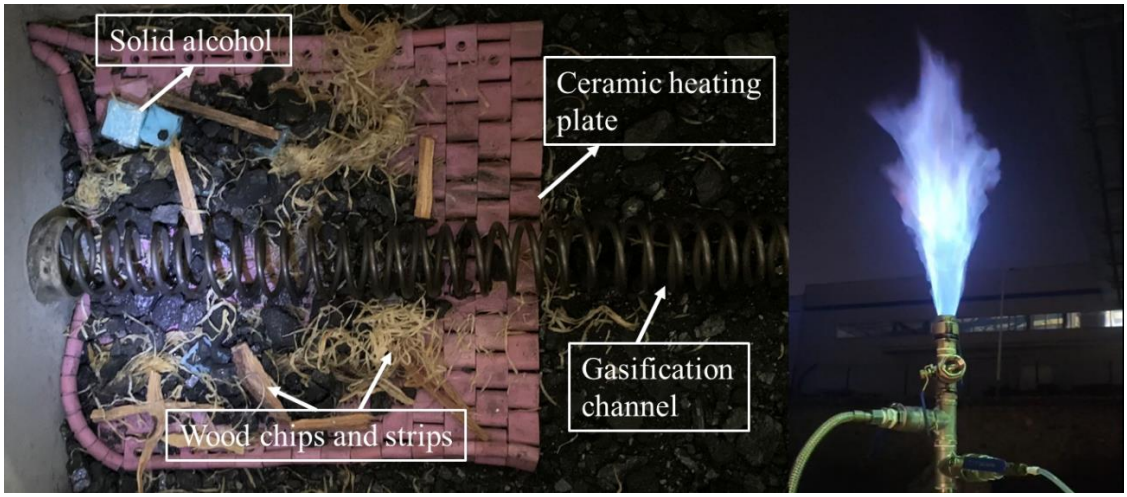

Figure 4. The laid ignition plate and the produced gas that successfully ignited

2.3 Experimental data monitoring

In the UCG process, the temperature distribution in the gasification zone can accurately reflect the experimental gasification process and help investigate the evolution of the gasification zone and the development and evolution of the coal combustion zone. Moreover, the layered temperature monitoring

method was adopted in this experiment. According to the height of the laid artificial coal seam, temperature sensors were installed in the layers with different burial depths so that the temperature distribution characteristics in the different height ranges from the gasification channel can be monitored in real time. The test system was equipped with ten type K thermocouples (Chino Corp) located on both sides of the gasification channel. The sensors T1-1—T1-5 are 60 mm above the gasification channel, the sensors T2-1—T2-5 are 310 mm above the gasification channel, and the interval between the axial sensors is 250 mm. The specific layout position is shown in Figure 5.

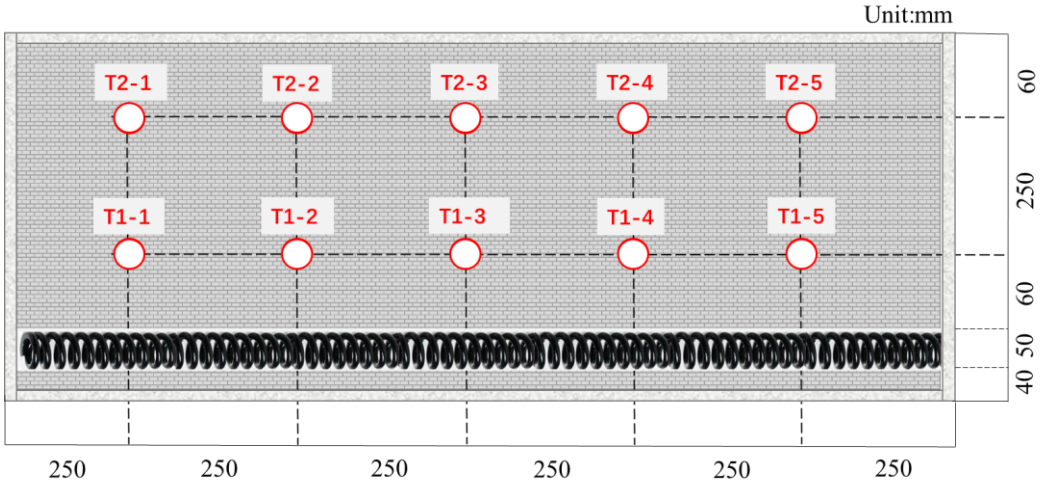

a) Side view

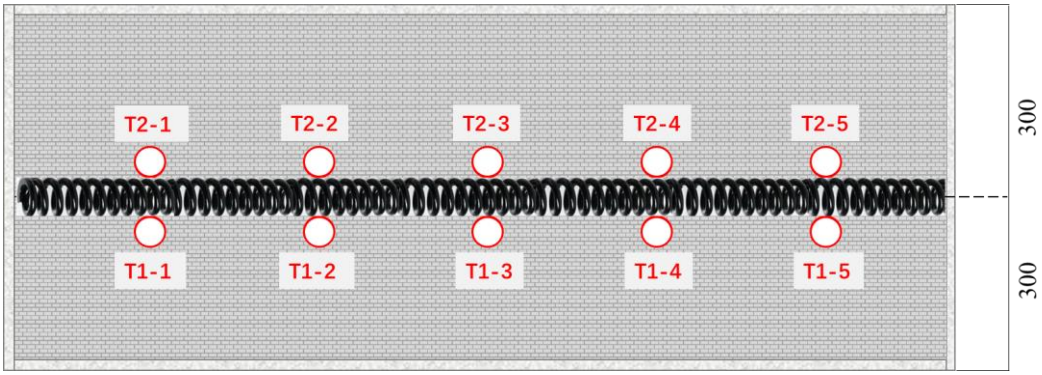

b) Vertical view

Figure 5. Deployment of thermocouples in the experimental reactor

3. Results and Discussion

3.1 Product gas compositions

Figure 6 shows the curves of change in composition and calorific value of the gas produced as a function of reaction time.

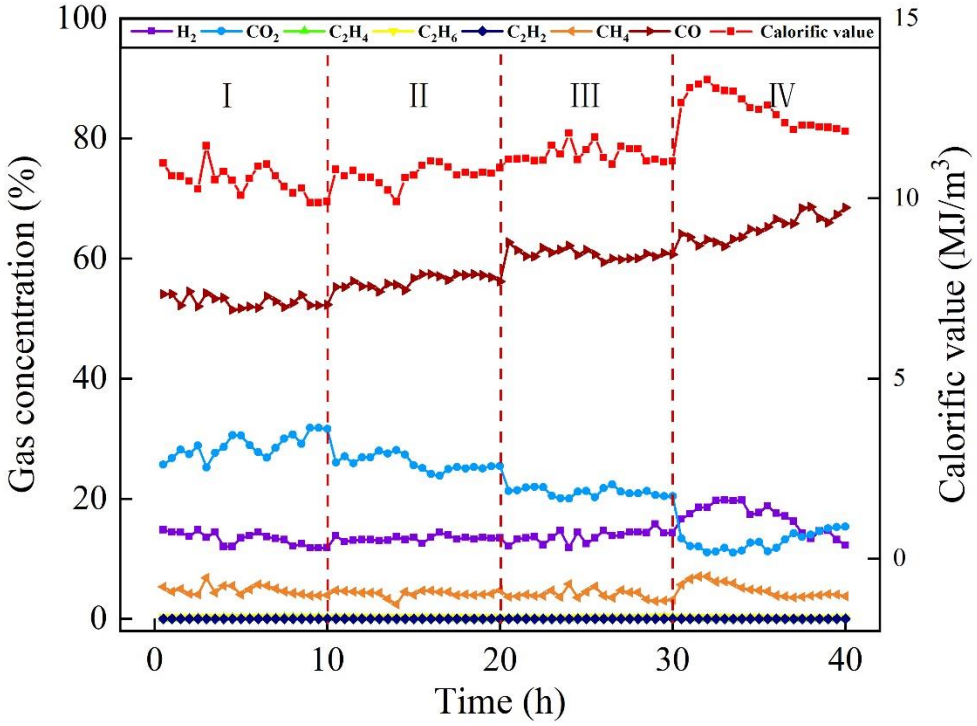

Figure 6. Changes in the calorific value and composition of the gas generated during gasification

By comparing and analyzing the generated gas concentrations in the four stages, the concentration of CO is closely related to the oxygen concentration. Because C+CO=2CO is a strongly endothermic reaction, the reaction equilibrium constant K_P increases sharply when the temperature rises. Thus, the higher the temperature is, the more conducive this temperature increase is to the reaction. With the increase in the oxygen concentration in the experimental model gasifier, the temperature in the gasifier increases. As a result, K_P increases, which is conducive to the reaction and finally increases the content of CO in the gas.

In the first three stages of the experiment, the change in the H_2 and CH_4 content in the generated gas composition was not apparent because the inherent moisture content of the coal sample is only 3.19%,

which is minimal. However, in the early phase of the fourth stage, the concentrations of H_2 and CH_4 significantly increased, possibly because refractory cement was used as the outer wall. During the later stage of the experiment, the combustion expanded to the outer wall. Therefore, the water in the material participated in the gasification process, which increased the H_2 content. H_2 is the primary reactant of the hydrogenation reaction ($C + 2H_2 = CH_4$), and, as a result, the concentration of CH_4 also began to rise. After rising for four hours, the concentrations of H_2 and CH_4 began to decrease, and the water in the outer wall of the cement had been consumed [34].

During the experiment, with the increase of oxygen concentration in the gasification agent, the concentration of the combustible gas in the produced gas and the calorific value of the produced gas show an upward trend. Because the calorific value of the produced gas is calculated according to the concentration of the combustible gas. The changing trend of the calorific value is very close to that of the CH_4 concentration because the heat of combustion of CH_4 is as high as 39.9 MJ/m^3, while the heat of combustion of CO and H_2 is only 12.6 MJ/m^3 and 12.8 MJ/m^3, respectively. Similarly, in the early period of the fourth stage of the experiment, the calorific value showed a significant upward fluctuation, which occurred because the content of CH_4 showed an apparent upward trend. Therefore, even if the proportion of the CH_4 content in the generated gas component is not very large, the influence on the calorific value is still significant.

Table 2. Gasification composition and calorific value

Component volume fraction (%)							Gas calorific value
H_2	CO_2	C_2H_4	C_2H_6	C_2H_2	CH_4	CO	(MJ/m^3)
13.29	28.77	0.11	0.24	0.03	4.75	52.81	10.48
13.35	24.93	0.04	0.24	0.08	4.21	57.15	10.66
13.75	21.04	0.08	0.23	0.02	4.10	60.78	11.26
17.44	12.22	0.02	0.20	0.07	4.92	65.13	12.48

The average concentration and average calorific value of the gas products in each stage are shown in

Table 2. The furnace temperature is low under low oxygen-rich conditions, and CO_2 does not participate effectively in the gasification reaction. Under higher oxygen-rich conditions, the furnace temperature is higher, which facilitates the CO_2 reduction reaction, and the CO content rises. Under the influence of high temperature, due to the release of a large amount of gas, shallow pore coal char is formed in the coal seam cracks, which provides more surface for combustion and gasification reactions [35]. Therefore, increasing the volume fraction of oxygen in the gasification agent can significantly increase the concentration of the combustible gas and improve the calorific value of the underground coal gasification system.

3.2 Temperature monitoring

The temperature field of coal seam and combustion zone affects whether the underground coal gasification can proceed smoothly. The change of temperature in the gasifier is a complex process that is related to a chemical reaction, heat conduction, heat radiation, and heat convection.

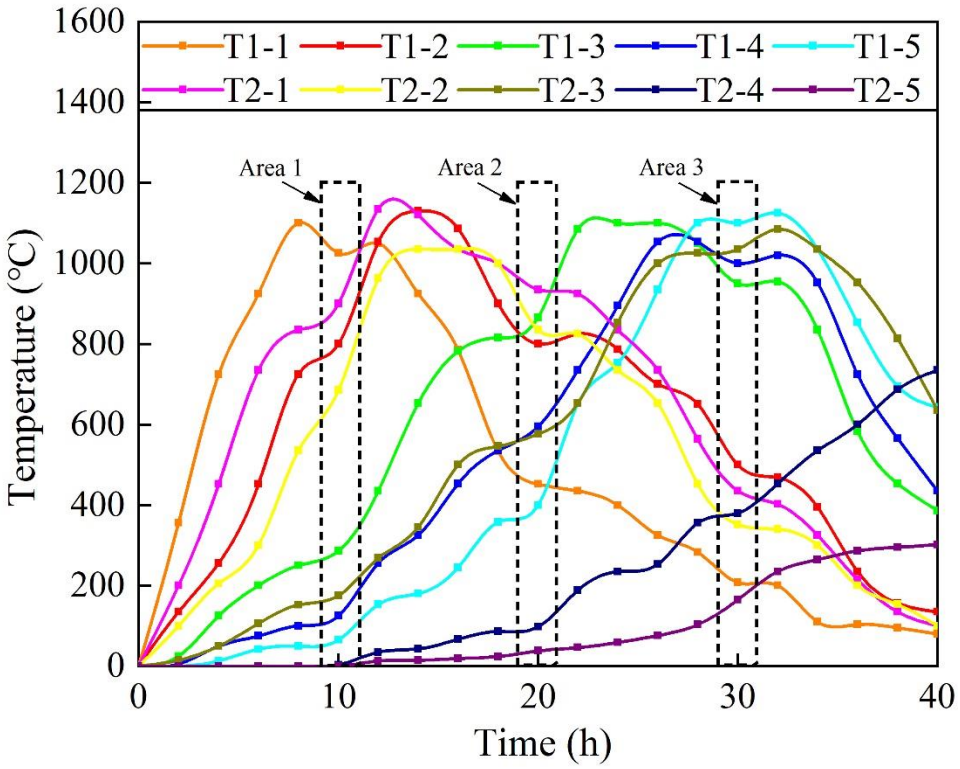

Figure 7. Temperature profiles

Figure 7 shows the curves of the temperature changes with time during the gasification process. The experimental results show that after the successful ignition of the gasifier, the temperature of the gasified coal seam rises sharply, and the influence range dramatically expands. The temperature of T1-1 rises to 1000°C first, which forms a high-temperature gasification chamber centered on the ignition hole. In the first three stages of the experiment, the temperature of the sensor that was located at the top of the gasification channel constantly changed before the temperature of the sensor that was near the gasification channel. The temperature of T2-1 that was above the ignition hole appeared to rise before the temperature of T1-2 that was in front of T2-1. Both temperatures of T2-2 and T2-3 that were in the middle and rear, respectively, appeared to rise before the temperatures of T1-3 and T1-4, which indicated that the temperature field mainly expanded radially along the gasification channel.

These results occurred because, when arranging the coal seam of the gasifier, the plane direction of the coal sample stratification was perpendicular to the gasification channel, and the propagation direction of the coal sample microcarack and crack tends to be parallel to the direction of the stratification plane [36]. The crack in the layer is the primary channel for the inward diffusion of the gasification agent in the initial stage of gasification. The surface with a crack has a larger specific surface area than the surface without a crack. Therefore, this surface can provide more active sites for combustion and gasification reactions. Thus, the combustion and gasification reaction in the coal seam fracture is more substantial than that in the channel.

When the experiment reaches the fourth stage, the temperature of T1-5 changes before the temperatures of T2-4 and T2-5, which indicates that the expansion direction of the coal seam temperature field begins to change. This result occurs because, as the oxygen concentration increases, which causes the coal seam cracking combustion and gasification reactions, excess oxygen begins to diffuse along the

gasification channel, and the surface reactions transpire at the coal walls of the gasification channel.

High-temperature gas diffusion along the channel, heat conduction, heat convection, and heat radiation work together. As a result, the temperature rises faster, which indicates that the temperature field mainly extends in the direction of the gasification channel. Furthermore, from areas 1, 2, and 3, whenever the oxygen concentration in the gasifier rises, the temperature rise rate becomes faster, and the fall rate slows down, which shows that the change in oxygen concentration can affect the trend of the temperature field in the gasifier.

3.3. Energy recovery evaluation

In the UCG process, the degree and rate of reaction are important parameters for efficient gasification, and the accurate calculation of gasification coal consumption is a prerequisite for determining the degree and rate of reaction. However, in practice, gasification coal consumption is not easy to observe and measure on site. Therefore, we propose a method to calculate the coal gasification amount based on carbon balance and provide an energy recovery for judging the gasification efficiency with the help of coal consumption.

3.3.1 Coal consumption of gasification

In the underground gasification process that is based on the conservation of elements in the chemical reaction process, the gasification consumption of coal can be estimated through the gas composition of the generated gas and the known reaction amount of O_2 in the gasification agent. The chemical reactions that occur during the underground gasification of coal can be expressed by the fundamental balance equation, as shown in Equation (1). Based on the results of the elemental analysis of coal, the chemical process can be fully discussed in terms of CH_mO_n, regardless of the specific structure of the coal sample composition.

$$CH_mO_n + \alpha O_2 + \beta H_2O \rightarrow \gamma H_2 + \sigma CO + \varepsilon CO_2 + \eta CH_4 \quad (1)$$

H_2, CO, CO_2 and CH_4 are assumed to be in the dry state, and the denitrogenated oxygen concentrations are p, q, r, and s, respectively. The parameters m and n can be derived from the elemental analysis of coal (m=H/C, n=O/C), where α and β are the equilibrium coefficients of O_2 and H_2O.

The total number of moles of the generated gas is assumed to be equal to Σ.

$$\Sigma = \gamma + \sigma + \varepsilon + \eta \tag{2}$$

The moles γ~η of each gas component are described as follows:

$$\gamma = p\Sigma; \sigma = q\Sigma; \varepsilon = r\Sigma; \eta = s\Sigma \tag{3}$$

$$p + q + r + s = 1 \tag{4}$$

By substituting these values into the carbon balance equation (σ+ε+η=1), the total number of moles Σ can be obtained as:

$$\sum = 1/(q + r + s) \tag{5}$$

Therefore, the following conclusions are drawn:

$$\begin{aligned} \gamma &= \frac{p}{q+r+s}; \sigma = \frac{q}{q+r+s} \\ \varepsilon &= \frac{r}{q+r+s}; \eta = \frac{s}{q+r+s} \end{aligned} \tag{6}$$

The decomposition of water β can be obtained by substituting Equation (6) into the hydrogen equilibrium equation (m+2β=2γ+4η) in Equation (1), as follows:

$$\beta = \frac{p+2s}{q+r+s} - \frac{1}{2m} \tag{7}$$

By substituting Equations (6) and (7) into the oxygen equilibrium equation (n+2α+β=σ+2ε) in Equation (1), the equilibrium coefficient α of O_2 is obtained as follows:

$$\alpha = \frac{q+2r-p-2s}{2(q+r+s)} + \frac{0.5m-n}{2} \tag{8}$$

The coal consumption A (kg/h) is determined by the O_2 consumption (Sm^3/h) and oxygen balance

coefficient α, as shown below:

$$A = \frac{S \times M \times 1.2 \times 1000}{22.4 \times C\% \times \alpha} \quad (9)$$

The term M is the mole fraction of O_2, and C% is the carbon content obtained by industrial analysis.

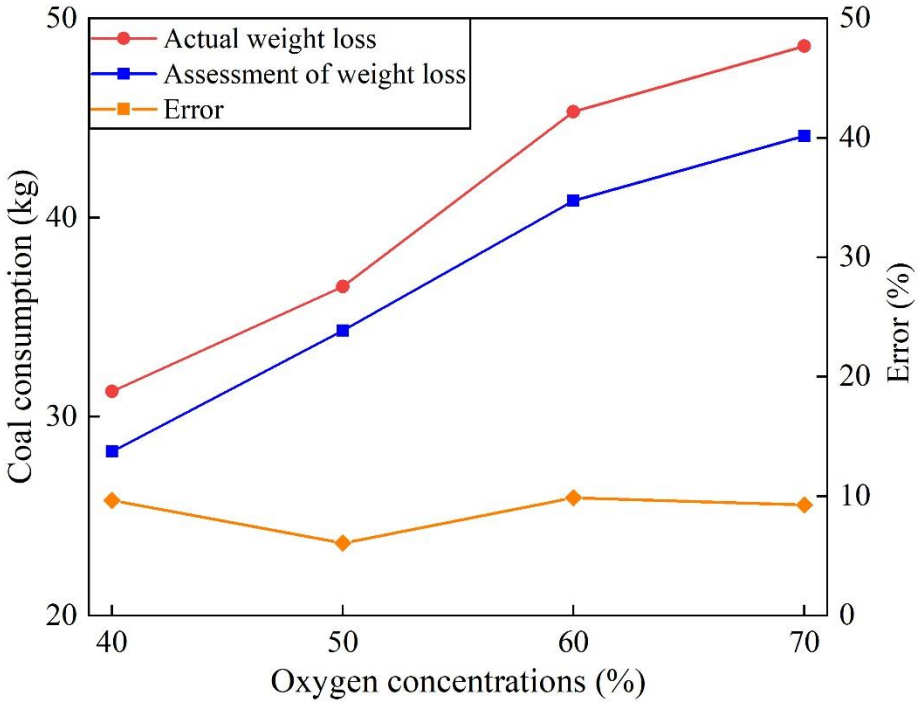

Figure 8. Actual values of model weight loss with estimated values

Figure 8 summarizes the coal consumption that was derived from the average gasification product composition at different gasification stages and the variation in the actual coal weight that was monitored according to the weighing system. Analysis of the data in this figure shows that the coal consumption increases with an increasing oxygen concentration, because as the oxygen concentration increases, the temperature in the gasification chamber increases, and the oxidation reaction in the gasifier occurs more intensely. As a result, more coal is consumed per unit time.

In this experiment, the actual monitored coal consumption was 161.72 kg, while the estimated coal consumption based on the conservation of carbon elements was 147.49 kg. The errors between the measured and estimated values in the four stages were 9.66%, 6.07%, 9.86%, and 9.27%, with an average

of 8.80%. All these error values were less than 10%, which proves that this theory can predict gasification coal consumption. Moreover, the error values may be caused by the evaporation of water from the coal (fissure free water), moisture from incompletely dried concrete, tar filtered by the filtration system, and volatile substances.

Figure 9 shows the actual coal consumption rates for the four stages. As seen from the figure 9, the oxygen concentration increases from 40% to 70%, and the coal consumption rate increases from 2.82 kg/h to 4.41 kg/h, which is an increase of 36.1%. The coal consumption rate can characterize the expansion progress in the combustion chamber; thus, increasing the oxygen concentration can promote the growth rate of the gasification chamber to advance and speed up the reaction process.

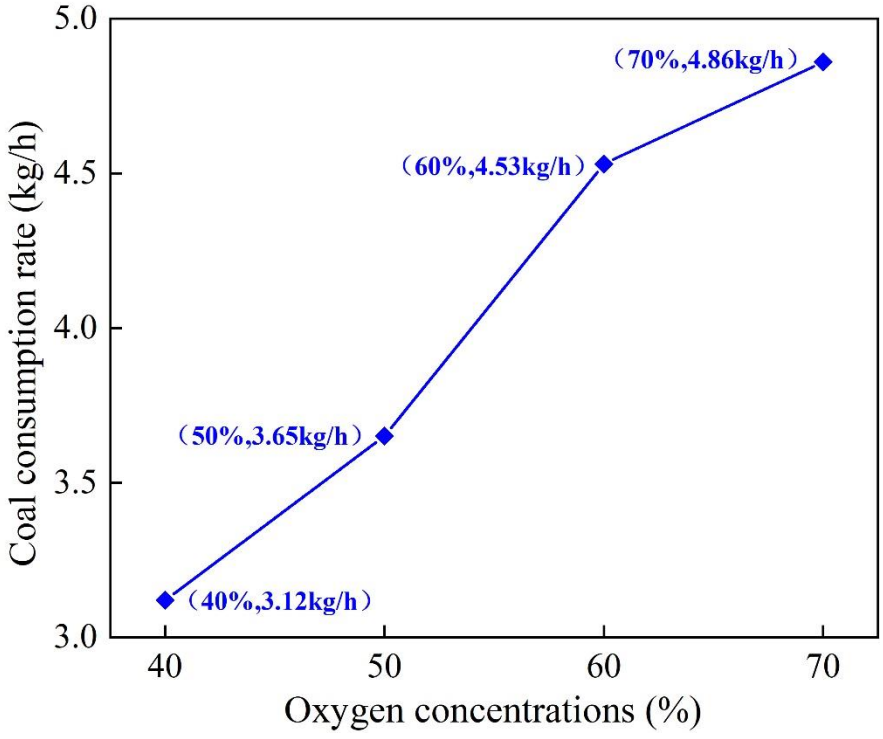

Figure 9. The change in the coal consumption rate at different stages

3.3.2 Energy recovery rate

During the underground gasification of coal, the gasification efficiency is usually judged by the conventional method of comparing the unit calorific value of gasification gas. However, this method

does not provide an accurate description of the efficiency. To further evaluate the gasification efficiency of the experiment, the author presents the definition of the energy recovery ratio (R_g), which is the ratio of the actual gas energy produced to the coal's heat generation. The calculation formula of this ratio is:

$$R_g = \frac{V_d \times \sum_{i=1}^{6} Q_i}{Q_c} \times 100\% \quad (10)$$

Where V_d is the unit gas yield of coal; Q_i is the unit gas calorific value of H_2, CH_4, CO, C_2H_2, C_2H_4, and C_2H_6; and Q_c is the unit calorific value of coal. According to Equation (10), the gasification efficiency of the four stages of this experiment was calculated, as shown in Table 3.

Table 3. Energy recovery rate of the UCG experimental model

Oxygen concentrations (%)	Gas production per unit coal (m^3/kg)	Gas calorific value (MJ/m^3)	Calorific value per unit coal (MJ/kg)	Energy recovery (%)
40	1.71	10.48	25.74	69.63
50	1.76	10.66	25.74	72.89
60	1.77	11.26	25.74	77.43
70	1.73	12.48	25.74	83.88

The experimental results show that the higher the percentage of oxygen in the injection flow is, the higher the gasification efficiency is. When the oxygen concentration increased from 40% to 70%, the energy recovery rate increased from 69.63% to 83.88%, which is an increase of 14.25%. This result implies that the high concentration oxygen injection conditions are beneficial to improving the coal gasification efficiency.

3.4 Temperature assessment modeling

The efficiency of the gasification process is related to the ratio and flow rate of the incoming gasifier and the reaction temperature inside the gasification chamber; although the temperature sensors were arranged in the gasification chamber, the temperature field distribution characteristics of the gasification chamber cannot be accurately obtained due to the limited number of sensors and the complex temperature

variation at each location and stage in the gasification chamber. Therefore, studying a means of estimating the gasification temperature is necessary. The relationship between the heat of reaction and sensible heat in the gasifier is shown in the following equation:

$$H_r = H_{sg} + H_{loss} \quad (11)$$

The reaction heat of gasification (H_r) is equal to the sum of the sensible heat of gas (H_{sg}) and the furnace heat loss (H_{loss}). Because this study added insulated concrete walls around the coal seam, the dissipated heat was ignored. Assuming that the gasifier in this experiment is an adiabatic reactor, the gasification temperature can be predicted based on the gas composition in the furnace.

The reaction equation when the coal is fully reacted is shown below:

$$CH_mO_n + (1 + 0.25m - 0.5n)O_2 + \beta H_2O \rightarrow CO_2 + (0.5m + \beta)H_2O \quad (12)$$

The combustion reaction of the gas is shown in the following equation:

$$\gamma H_2 + \sigma CO + \eta CH_4 + (0.5\alpha + 0.5\sigma + 2\eta)O_2 \rightarrow CO_2 + (0.5m + \beta)H_2O \quad (13)$$

According to Equation (1), (12) and (13), the following calculation can be obtained from the heat of reaction (The coefficients of Equations (14-17) can be found in the relevant literature data):

$$Hr = hcoal - (\gamma hH_2 + \sigma hCO + \eta hCH_4) \quad (14)$$

The calorific value of the gas in Equation (14) is shown in Table 4.

Table 4. Heat of combustion of gas

Gas	Value (MJ/m^3)
H_2	12.8
CO	12.6
CH_4	39.9

The sensible heat of the gas is calculated by the following equation:

$$H_{sg} = N \times C_p \times T \quad (15)$$

In this equation, N is the number of moles of the gas, C_P is the specific heat capacity of the gas. The

335 total sensible heat of each component is determined by comparing the sensible heat of the generated gas

336 H_{sg} and the heat of reaction H_r. When $H_{sg} \neq H_r$, T is reassumed, and the estimation is repeated until $H_{sg}=H_r$;

337 then, the temperature is the gasification temperature. The specific heat capacity of the gas also changes

338 with temperature, and the formula for calculating the specific heat capacity is as follows:

$$Cp = a + bT + cT^2 + dT^3 \quad (16)$$

339 Table 5 shows the parameters that are used to calculate the specific heat capacity of the gas at different

340 temperature states.

Table 5. Specific heat capacity parameters

Gas composition	a	$b\times10^2$	$c\times10^5$	$d\times10^9$
H_2	6.952	-0.04576	0.09563	-0.2079
CO	6.726	0.04001	0.12830	-0.5307
CO_2	5.316	1.4285	-0.8362	1.7840
CH_4	4.750	1.200	0.303	-2.630
N_2	6.903	-0.03753	0.1930	-0.6861
H_2O	7.700	0.04594	0.2521	-0.8387

341 Therefore, the sensible heat of each gas component is:

$$Hsg = \int_{25}^{T} (a + bT + cT^2 + dT^3) dT \quad (17)$$

342 The gas composition monitored at the outlet at a certain moment can be regarded as the average value

343 of the gas composition in the furnace; thus, the calculated gasification temperature is the average

344 gasification temperature in the furnace. Figures 10-13 show the measured (>550°C), estimated and

345 estimated error values of the temperature in the high-temperature gasification region for the four stages

346 of this test.

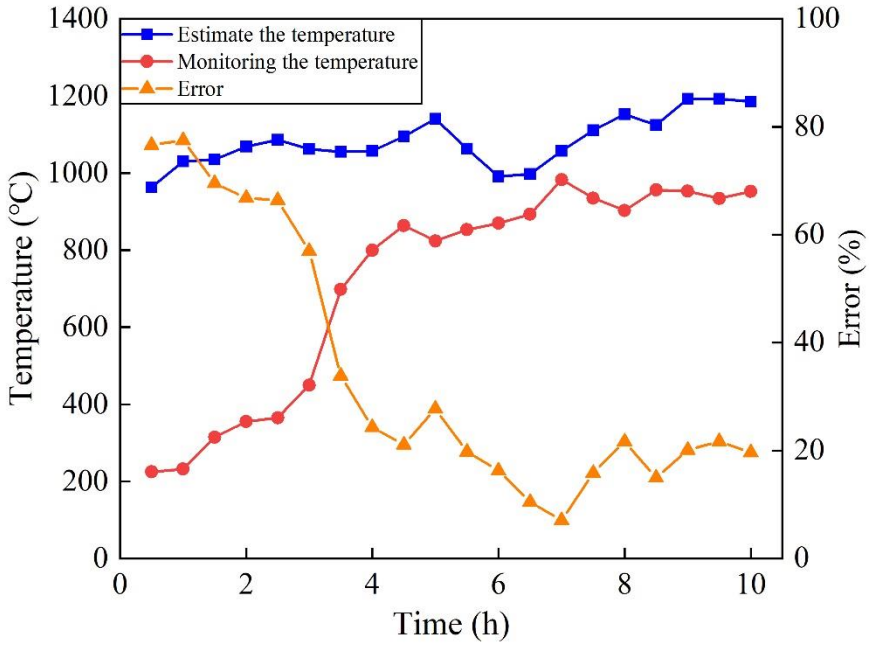

347

348 **Figure 10.** The monitored temperature and estimated temperature change with time

349 (40% oxygen concentration)

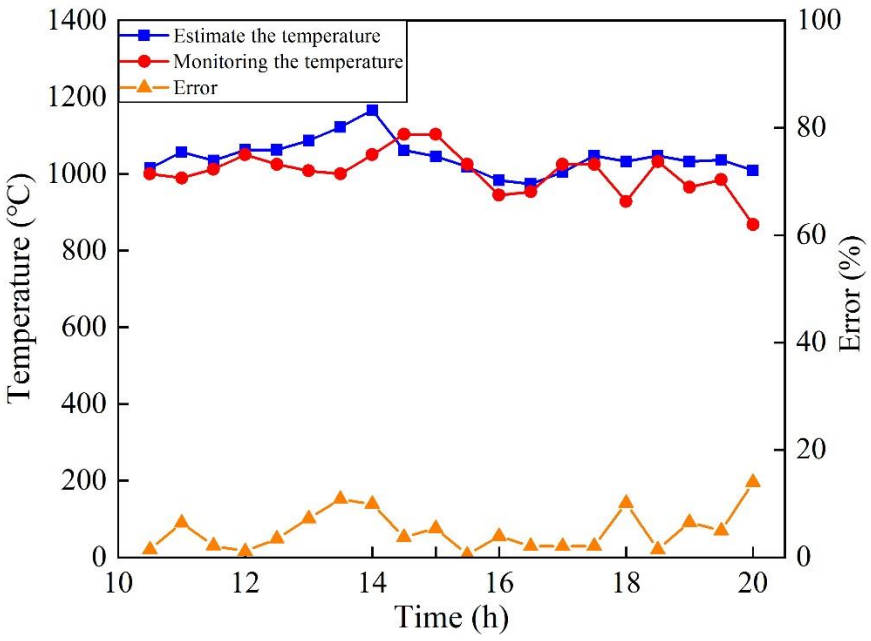

350

351 **Figure 11.** The monitored temperature and estimated temperature change with time

352 (50% oxygen concentration)

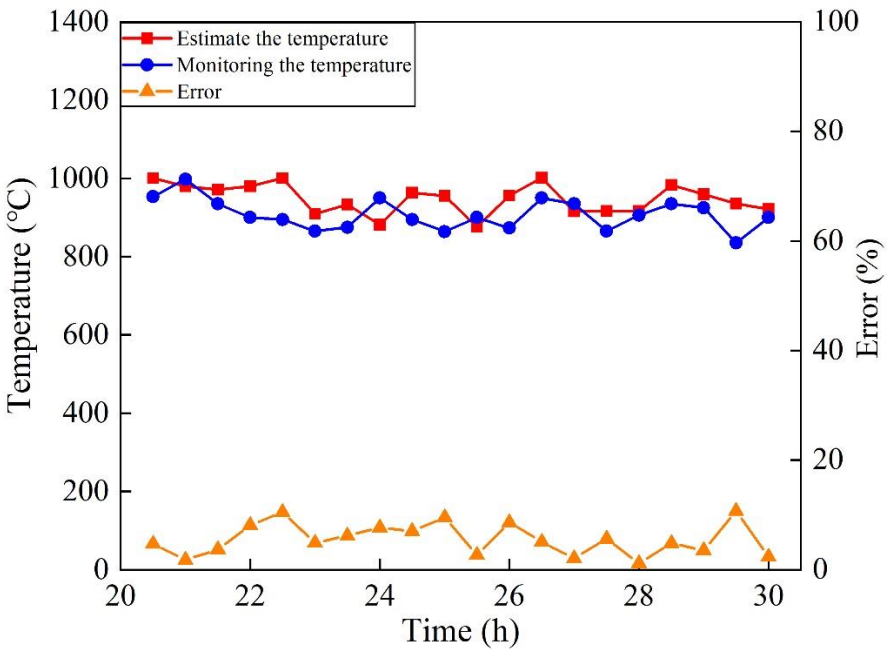

353

354 **Figure 12.** The monitored temperature and estimated temperature change with time

355 (60% oxygen concentration)

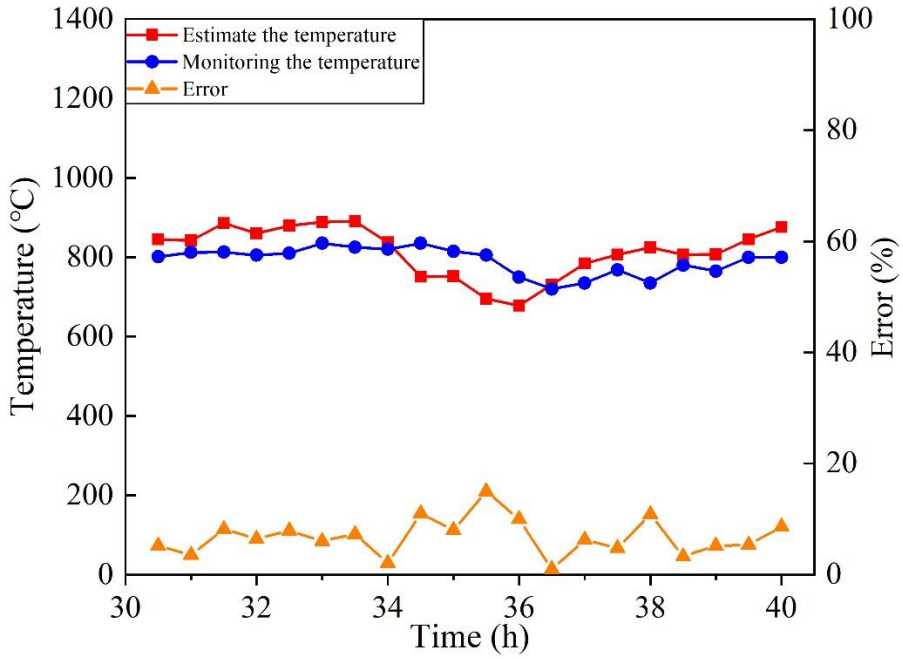

356

357 **Figure 13.** The monitored temperature and estimated temperature change with time

358 (70% oxygen concentration)

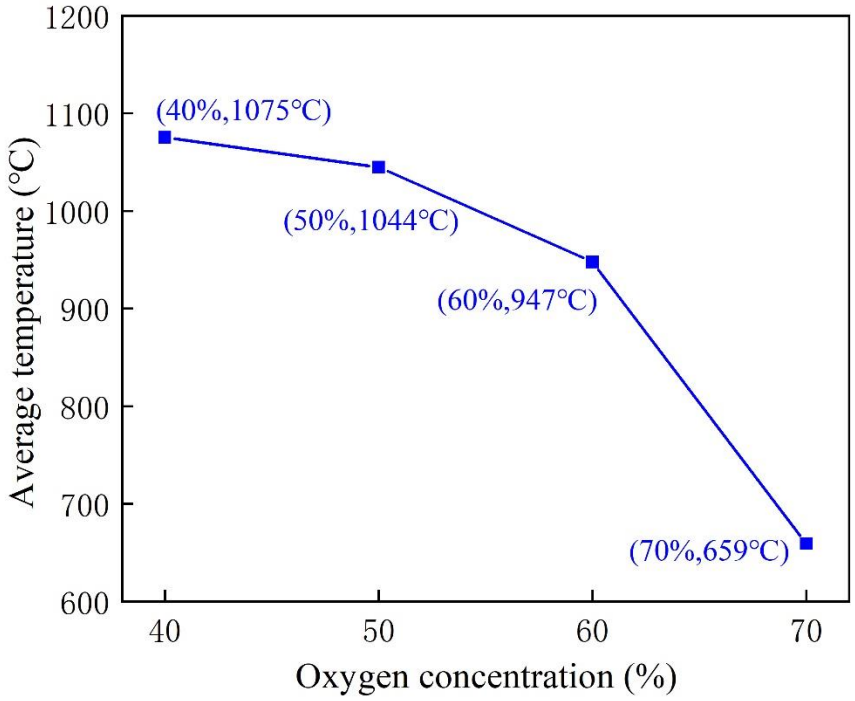

Figure 14. The change in average temperature at different stages

In the beginning of this experiment, the temperature in the furnace was low because the experiment was in the ignition and heating stage. This state was suitable for the dry distillation reaction of coal to proceed. Combustible gases such as CH_4 and H_2 were released from the coal samples around the gasification channel. The calculated temperature was high, so the error between the two kinds was large. After three hours of the experiment, as the temperature of the gasification zone rises, the oxidation and reduction zones began to occupy the main body. The error also began to drop significantly, but still remained at about 20%. This is because the gasification cavity formed at the early stage of gasification is small and the temperature distribution is concentrated and not uniform, so averaging the monitored temperature above 600°C will keep the temperature at a relatively low level; as a result, the error at this stage was large. In the second stage of the experiment, with the gradual expansion of the gasification chamber, the distribution of high-temperature areas became uniform, and the error gradually decreased. The average error in this stage was only 5.32%, while the average errors in the third and fourth stages,

which were both stable at approximately 5%, were 5.56% and 6.80%, respectively. As viewed from all four stages, the estimated temperature was slightly higher than the monitored value overall. This result occurred because the sensible heat value rose due to the lack of the heat loss in the gasifier when calculating the temperature in the gasification section; thus, the estimated temperature was calculated to be on the high side. At some times, such as during the timeframes of 14.5 h-15.5 h in the second stage and 24 h in the third stage, the monitored value was slightly higher than the estimated value. This maybe due to the collapse of the coal seam above the gasification zone, which leads to the increase in the contact face value between the coal sample and the gasification agent. Therefore, the temperature in the gasifier rises rapidly. By calculating the average temperature of the gasification zone (Figure 14), we also found that the gasification temperature showed a downward trend, which indicated that the ratio of the reduction zone to the oxidation zone gradually increased. However, in the fourth stage of the experiment, the gasification temperature was within the temperature range of the reduction zone, between 550 ℃ and 900 ℃, which indicates that the reduction zone occupied the main body of the gasifier. Therefore, we can improve the gasification efficiency by increasing the oxygen concentration. The actual monitored temperatures in the four stages are consistent with the estimated temperature change trend, which proves that this theory can estimate the high-temperature range in the gasification chamber.

Figure 15 shows the relationship between the temperature and heat of reaction for the four stages deduced from this experiment. Fitting the temperature to the heat of reaction data revealed that the heat of reaction was linearly correlated with temperature, and the correlation coefficient was as high as 0.99, which demonstrates this method's reliability.

393

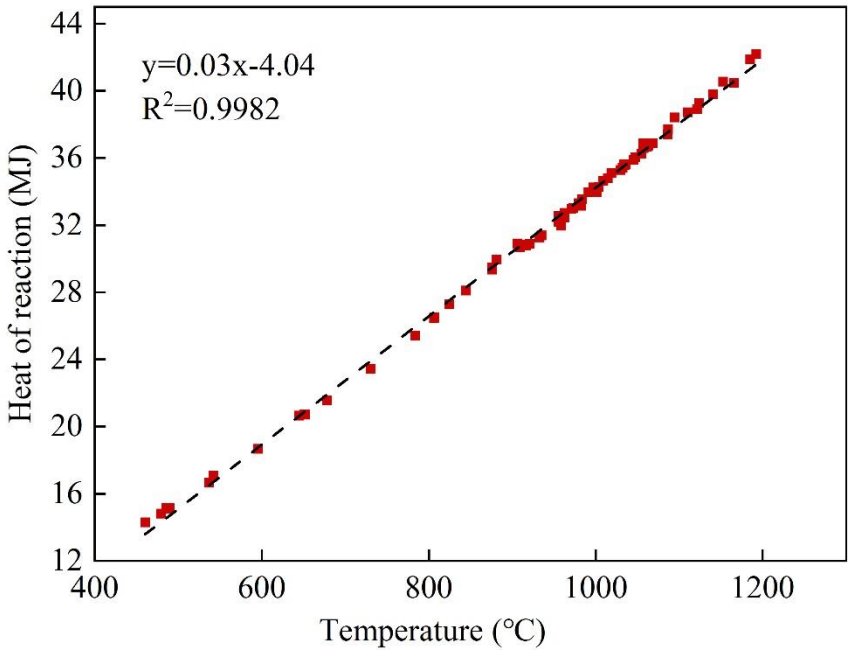

394 **Figure 15.** Change of the heat of reaction with temperature

395 **4. Discussion**

396 The gasification agent in this experiment was oxygen-rich air, and no water vapor was added. The H_2
397 and CH_4 in the gasification products mainly came from the water and hydrogen-containing compounds
398 in the coal samples. The rise in H_2 and CH_4 content in the early part of the fourth stage is probably due
399 to the participation of water in the refractory cement in the gasification reaction. This paper established
400 a theoretical calculation method of coal consumption in the gasification process based on carbon balance.
401 Comparing the actual coal consumption in the test process, the estimated value that is calculated by using
402 this method is 8.7% higher, which may be caused by the evaporation of water from the coal samples as
403 well as from the external concrete, the tar filtered by the filtration system, and the presence of volatile
404 substances. The temperature trend of the whole gasification process can be estimated more accurately
405 based on the heat balance theory. When comparing the estimated value with the monitored value, the
406 estimated value was slightly higher than the monitored value. When estimating the gasification interval
407 temperature, the heat loss in the gasifier was ignored, which increased the estimated sensible heat value.

Therefore, the estimated temperature will rise accordingly. In the later stage, we can add a thermal insulation layer to the gasifier to reduce heat loss and improve the estimation accuracy. However, considering the buried depth of the coal seam in the field experiment, this problem can be solved. In the following study, we will consider the coal seam's dip angle and burial depth to ensure the similarity between the simulation experiment and the field experiment.

5. Conclusion

(1) The volume fraction of oxygen in the gasification agent is one of the main factors that affect the gasification effect. Increasing the oxygen concentration in the gasifier can significantly increase the proportion of combustible gases in the output gas. When the oxygen concentration increased from 40% to 70%, the calorific value of the product gas increased from 10.48 MJ/m^3 to 12.48 MJ/m^3. The experiment conducted demonstrated that the oxygen-enriched air as react gas for sustaining the gasification process is a feasible option.

(2) For UCG field experiments, coal consumption cannot be measured directly. Thus, establishing a model to estimate the coal consumption for UCG experiments is crucial. For this UCG simulation experiment, we compared the theoretically calculated coal consumption with the actual experimental results. The actual value was 161.72 kg and the theoretical estimated value was 147.49 kg. The error percentage was not more than 10%, which indicates that the coal consumption in the gasification process can be estimated by this method.

(3) The evaluation of gas recovery is the reverse deduction of the experimental results from the chemical point of view, so as to evaluate the gasification reaction process. When the volume concentration of injected oxygen increased from 40% to 70%, the energy recovery rate increased from 69.63% to 83.88%. Increasing the volume concentration of the gasifier oxygen can significantly improve

the gasification efficiency of the underground coal gasification system.

(4) Based on the output gas composition, an evaluation model of the underground gasification temperature field of coal was developed by combining the law of thermodynamic conservation. The temperature of the gasification chamber at each stage was evaluated by calculating the reaction heat and sensible heat. After gasification stabilization, the error values of the actual monitored temperature and the theoretical estimated temperature were 5.32%, 5.56% and 6.80%, respectively, which indicates that this theory may be helpful for estimating the temperature of the gasification zone.

Declaration of Competing Interest

The authors declare that they have no known competing financial interests or personal relationships that could have appeared to influence the work reported in this paper.

Acknowledgments: This work was supported by Key Laboratory of Western Mine Exploitation and Hazard Prevention, Ministry of Education (SKLCRKF1902), State Key Laboratory for Geomechanics and Deep Underground Engineering, China University of Mining & Technology (SKLGDUEK2004), Key R & D and promotion projects in Henan Province (16220043), Henan Province Key Scientific Research Project Plan for Colleges and Universities (22B440003).

References

[1] Laciak M, Chen ME. Modeling and control of energy conversion during underground coal gasification process. Energies 2022;15. https://doi.org/10.3390/en15072494.

[2] Qian MG, Jia-Lin XU, Miao XX. Green technique in coal mining. Journal of China University of

Mining & Technology 2003;32(4):344-8. https://doi.org/10.3321/j.issn:1000-1964.2003.04.001.

[3] Bazaluk O, Lozynskyi V, Falshtynskyi V, Saik P, Cabana E. Experimental studies of the effect of design and technological solutions on the intensification of an underground coal gasification process. Energies 2021;14(4):4369. https://doi.org/10.3390/en14144369.

[4] Zhao B, Dong X, Chen Y, Chen S, Chen Z, Peng Y, et al. Experimental investigation on the pore structure evolution of coal in underground coal gasification process 2022. https://doi.org/10.1021/ACSOMEGA.2C00157.

[5] Hu Z, Peng Y, Sun F, Chen S, Zhou Y. Thermodynamic equilibrium simulation on the synthesis gas composition in the context of underground coal gasification. Fuel 2021;293:120462. https://doi.org/10.1016/j.fuel.2021.120462.

[6] Khadse A, Qayyumi M, Mahajani S, Aghalayam P. Underground coal gasification: a new clean coal utilization technique for india. Energy 2007. https://doi.org/10.1016/j.energy.2007.04.012.

[7] Chiesa P, Consonni S, Kreutz T, Williams R. Co-production of hydrogen, electricity and CO_2 from coal with commercially ready technology. Part a: performance and emissions. Int J Hydrogen Energ 2005;30(7):747-67. https://doi.org/10.1016/j.ijhydene.2004.08.002.

[8] Grabowski J, Korczak K, Tokarz A. Aquatic risk assessment based on the results of research on mine waters as a part of a pilot underground coal gasification process. Process Saf Environ 2021;148:548-58. https://doi.org/10.1016/j.psep.2020.10.003.

[9] Pivnyak G, Falshtynskyi V, Dychkovskyi R, Saik P, Koshka O. Conditions of suitability of coal seams for underground coal gasification. Key Engineering Materials 2020;844:38-48. https://doi.org/10.4028/www.scientific.net/KEM.844.38.

[10] Mandal R, Maity T, Chaulya SK, Prasad GM. Laboratory investigation on underground coal gasification technique with real-time analysis. Fuel 2020;275:117865. https://doi.org/10.1016/j.fuel.2020.117865.

[11] Wiatowski M, Kapusta K. Evolution of tar compounds in raw gas from a pilot-scale underground coal gasification (ucg) trial at wieczorek mine in poland. Fuel 2020;276:118070. https://doi.org/10.1016/j.fuel.2020.118070.

[12] Daggupati S, Mandapati RN, Mahajani SM, Ganesh A, Mathur DK, Sharma RK, et al. Laboratory studies on combustion cavity growth in lignite coal blocks in the context of underground coal gasification. Energy 2010;35(6):2374-86. https://doi.org/10.1016/j.energy.2010.02.015.

[13] Selivanova T, V VP, School E. Thermo-chemical conversion of coal samples under high temperature. https://doi.org/10.3969/j.issn.1673-9736.2013.03.03.

[14] Pei P, Nasah J, Solc J, Korom SF, Laudal D, Barse K. Investigation of the feasibility of underground coal gasification in north dakota, united states. Energy Convers Manage 2016;113(Apr.):95-103. https://doi.org/10.1016/j.enconman.2016.01.053.

[15] Vairakannu P, Kumari G. CO_2 enhanced in-situ oxy-coal gasification based carbon-neutral conventional power generating systems. Journal of Energy 2015;84:672-83. https://doi.org/10.1016/j.energy.2015.03.029.

[16] Liu H, Liu S. Exergy analysis in the assessment of hydrogen production from ucg. Int J Hydrogen Energ 2020;45(51):26890-904. https://doi.org/10.1016/j.ijhydene.2020.07.112.

[17] Andrianopoulos E, Korre A, Durucan S. Chemical process modelling of underground coal gasification and evaluation of produced gas quality for end use. Energy Procedia 2015;76:444-

53. https://doi.org/10.1016/j.egypro.2015.07.870.

[18] Zagorak R, Sadasivam S, Thomas HR, Stańczyk K, Kapusta K. Experimental study of underground coal gasification (ucg) of a high-rank coal using atmospheric and high-pressure conditions in an ex-situ reactor. Fuel 2020;270:117490. https://doi.org/10.1016/j.fuel.2020.117490.

[19] Smoliński A, Stańczyk K, Kapusta K, Howaniec N. Chemometric study of the ex situ underground coal gasification wastewater experimental data. Water, Air, & Soil Pollution 2012;223(9):5745-58. https://doi.org/10.1007/s11270-012-1311-5.

[20] Otto C, Kempka T. Synthesis gas composition prediction for underground coal gasification using a thermochemical equilibrium modeling approach. Energies 2020;13. https://doi.org/10.3390/en13051171.

[21] Klebingat S, Kempka T, Schulten M, Azzam R, Fernández-Steeger TM. Optimization of synthesis gas heating values and tar by-product yield in underground coal gasification. Fuel 2018;229:248-61. https://doi.org/10.1016/j.fuel.2018.02.039.

[22] Perkins G, Vairakannu P. Considerations for oxidant and gasifying medium selection in underground coal gasification. Fuel Process Technol 2017;165:145-54. https://doi.org/10.1016/j.fuproc.2017.05.010.

[23] Wang J, Wang Z, Xin L, Xu Z, Gui J, Lu X. Temperature field distribution and parametric study in underground coal gasification stope. Int J Therm Sci 2017;111:66-77. https://doi.org/10.1016/j.ijthermalsci.2016.08.012.

[24] Gur M, Eskin N, Okutan H, Arısoy A, Böke E, Altıntaş Ü, et al. Experimental results of underground coal gasification of turkish lignite in an ex-situ reactor. Fuel 2017;203:997-1006.

https://doi.org/10.1016/j.fuel.2017.03.008.

[25] Massaquoi J, Riggs JB. Mathematical modeling of combustion and gasification of a wet coal slab-I: Model development and verification. Chemical Engineering Science 1983;38(10):1747-56. https://doi.org/10.1016/0009-2509(83)85031-3.

[26] Yang L. The dynamic temperature field of two-stage underground coal gasification (ucg). Energy Sources 2006;28(4/8):667-80. https://doi.org/10.1080/009083190951438.

[27] Xi J, Liang J, Sheng X, Shi L, Li S. Characteristics of lump lignite pyrolysis and the influence of temperature on lignite swelling in underground coal gasification. J Anal Appl Pyrol 2016;117(Jan.). https://doi.org/10.1016/j.jaap.2015.11.011.

[28] Yang D, Sarhosis V, Sheng Y. Thermal–mechanical modelling around the cavities of underground coal gasification. J Energy Inst 2014;87(4):321-9. https://doi.org/10.1016/j.joei.2014.03.029.

[29] Prabu V, Jayanti S. Heat-affected zone analysis of high ash coals during ex situ experimental simulation of underground coal gasification. Fuel 2014;123:167-74. https://doi.org/10.1016/j.fuel.2014.01.035.

[30] Kapusta K, Stańczyk K, Wiatowski M, Chećko J. Environmental aspects of a field-scale underground coal gasification trial in a shallow coal seam at the experimental mine barbara in poland. Fuel 2013;113:196-208. https://doi.org/10.1016/j.fuel.2013.05.015.

[31] Liu HT, Yao H, Yao K, Chen F, Luo GQ. Characteristics of "three zones" during underground coal gasification. Advanced Materials Research 2012;524-527:56-62. https://doi.org/10.4028/www.scientific.net/AMR.524-527.56.

[32] Liu H, Feng C, Xia P, Kai Y, Liu S. Method of oxygen-enriched two-stage underground coal

gasification. Mining Science and Technology (China) 2011;21(2):191-6. https://doi.org/10.1016/j.mstc.2011.02.018.

[33] Wang Z, Huang W, Zhang P, Xin L. A contrast study on different gasifying agents of underground coal gasification at huating coal mine. Journal of Coal Science and Engineering (China) 2011;17(2):181-6. https://doi.org/10.1007/s12404-011-0214-1.

[34] Hamanaka A, Su F, Itakura K, Takahashi K, Kodama J, Deguchi G. Experimental study on evaluation of underground coal gasification with a horizontal hole using two different coals. Fuel 2021;305:121556. https://doi.org/10.1016/j.fuel.2021.121556.

[35] Wang Z, Wei Y, Hou T, Jin Y, Wang C, Liang J. Large-scale laboratory study on the evolution law of temperature fields in the context of underground coal gasification. https://doi.org/10.1016/j.cjche.2020.07.005.

[36] Su FQ, Itakura KI, Deguchi G, Ohga K. Monitoring of coal fracturing in underground coal gasification by acoustic emission techniques. Appl Energ 2017;189(MAR.1):142-56. https://doi.org/10.1016/j.apenergy.2016.11.082.

Energy recovery evaluation and temperature field research of underground coal gasification under different oxygen concentrations

Fa-qiang Su[a,b], Tao-Zhang[a], Jun-bo Wu[a], Qi-chao Deng[a], Akihiro Hamanaka[c], Yi-he Yu[a,b,*] Meng-jia Dai[a], Xiao-long He[a], Jun-nan Yang[a]

[a] *School of Energy Science and Engineering, Henan Polytechnic University, Jiaozuo, Henan, 454-003, China*

[b] *State Collaborative Innovation Center of Coal Work Safety and Clean-efficiency Utilization, Henan Polytechnic University, Jiaozuo, Henan, 454-003, China*

[c] *Department of Earth Resources Engineering, Kyushu University, 744 Motooka, Nishi-ku, Fukuoka 819-0395, Japan*

* *Correspondence: yyhcmsj@hpu.edu.cn*

Abstract：

In this paper, UCG simulation experiments were carried out on selected coal samples to study the effects of the gasification agent ratio on the product gas composition and calorific value under different oxygen concentrations. Moreover, an energy recovery evaluation method based on stoichiometric theory was established based on the carbon (C) balance in the generated gas content, and the energy recovery rate and coal consumption of the underground gasification process were evaluated. Based on the composition of the produced gas and the thermodynamic law of conservation, an evaluation model of the underground coal gasification temperature field was established. The gasification chamber temperature in each stage was evaluated by calculating the reaction heat and sensible heat. The experimental and

research results showed that when the volume fraction of oxygen in a gasification agent was in the range 40 - 70 % and the calorific value of the produced gas increased from 10.48 MJ/m^3 to 12.48 MJ/m^3. The calorific value of the produced gas increased with an increasing oxygen concentration. Furthermore, the energy recovery rate increased from 69.63% to 83.88%, indicating that the gasification efficiency of the UCG experiment can be significantly improved with an increasing oxygen concentration. The error between the theoretical value of the coal consumption and the actual monitoring value was within 10%, which effectively evaluates the coal consumption in the gasification process. The theoretical calculation temperature was consistent with the experimental monitoring temperature results, and the reaction heat was found to also be linearly correlated with the gasification temperature. Therefore, this method can effectively determine the gasification chamber temperature. These monitoring and evaluation methods are expected to guide the analysis of subsurface field experiments.

Keywords: Underground coal gasification; Stoichiometry; Coal consumption; Gasification efficiency; Sensible heat

1. Introduction

Underground coal gasification is a complex physicochemical change process that involves heat and mass transfer, fluid flow, gas–solid two-phase chemical reactions, and other problems [1-3]. Compared with traditional coal mining methods, underground coal gasification is not only suitable for the mining of deep, steep, and gently inclined coal seams but can also reduce the mining cost and damage to the environment, which is consistent with the national construction of a low-carbon, clean, safe and efficient modern energy system [4,5].

Underground coal gasification is an industrial means to burn coal resources in situ by injecting gasification agents such as O_2, H_2O and CO_2 to obtain combustible gases such as CH_4, H_2 and CO [6,7]. The coal seam steadily burns when heated, and the underground fire area gradually expands, forming a gradient temperature field [8,9]. The chemical reaction process presents different reaction phenomena under different temperature conditions. Therefore, the following three reaction zones are formed in the

gasification channel: the oxidation zone, reduction zone, and dry distillation zone. Figure 1 shows the temperature range of each reaction zone and the main chemical reactions in the underground coal gasification [10,11].

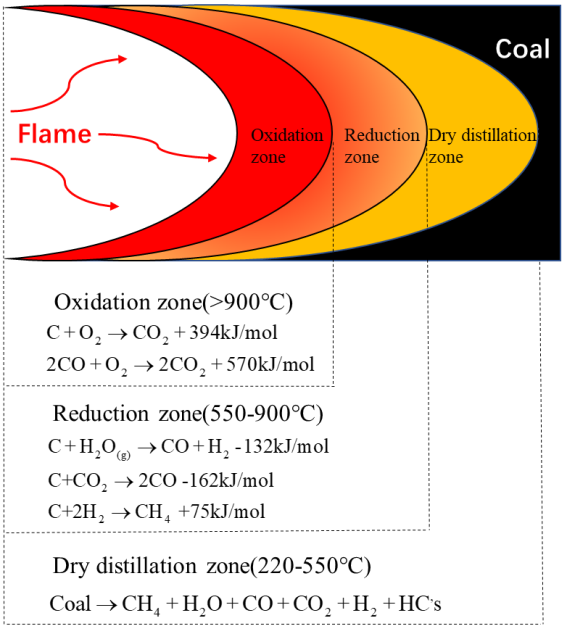

Figure 1. Three zones in the underground coal gasification

The temperature in the oxidation zone usually is higher than 900°C, which is the heat source that promotes the gasification process. The main chemical reactions that produce combustible gases in the UCG process occur in the reduction and dry distillation zones. In terms of the chemical reactions, the three zones are not strictly delineated, but rather the relative strengths and weaknesses of the redox and dry distillation reactions are elaborated [12].

The underground gasification process of coal is complex, and the process flow is unique [13-15]. Currently, scholars in this field have conducted research on the development of gasification cavities, the efficiency of gasification and its influencing factors, and the analysis of the gasification process based on chemical methods. To optimize the efficiency of energy conversion in the process of underground coal gasification, Shuqin Liu and others [16] established an exergy evaluation model of an underground

63 coal gasification system in combination with the first law of thermodynamics and the second law of
64 thermodynamics. E. Andrianopoulos [17] combined chemical process modeling with a UCG-specific
65 underground layout to evaluate the quality of the syngas produced. Renato Zagorščak [18]
66 experimentally investigated the effects of different pressures and gasification agent ratios on the
67 gasification process. Adam Smoliński [19] analyzed and studied the harmful inorganic substances in the
68 wastewater that was produced in the process of underground coal gasification by chemical methods.
69 However, there are relatively few theoretical and experimental studies that is based on the chemometrics
70 theory to evaluate the energy recovery in the whole process of underground coal gasification.
71 Additionally, accurate methods that are generally suitable for evaluating the efficiency of underground
72 coal gasification are lacking.

73 Gasification agents with different oxygen concentrations directly affect the temperature of the
74 gasification area, while the UCG process is a self-heat balance process [20]. The heat generated by
75 combustion is conducive to establishing the ideal temperature field of the underground gasifier and leads
76 to a reduction reaction and decomposition reaction, which finally produces gas [21]. Therefore, in the
77 UCG process, mastering the temperature field distribution law of the UCG extraction field is not only
78 crucial for further research on the development of the combustion void zone and the structure and size
79 parameters of the gasifier, but also provide meaningful guidance for the improvement in gasification
80 technology and the development of combustion control technology [22-24]. The dynamic evolution of
81 the temperature field affects the stability of the underground coal gasification process; thus, many
82 researchers are attentive to the research of the temperature field. By considering the wet coal area and
83 dry distillation area, Massaquoi and Riggs [25] established a one-dimensional mathematical model to
84 predict the combustion process of underground coal gasification. Based on the model test, Lanhe Yang

[26] established a two-dimensional linear dynamic mathematical model of the temperature field of the gasification layer, and calculated the parameters by the control volume method. In addition, the calculated values that were obtained by the model are consistent with the measured values. Jianfen Xi and others [27] used Ulanqab lignite to study the dynamic expansion of the underground coal seam temperature field, and concluded that the expansion of the temperature field is mainly affected by the coal seam fissures and gasification agent flow. With the in-depth study of underground coal gasification, the temperature field is developing in the direction of the mechanism, three dimensions and whole process. After years of research and field practice, underground coal gasification technology has achieved remarkable results. Due to the complexity and invisibility of underground coal gasification, attaining long-term stable production and commercial development still needs further research and improvement [28-33].

This underground coal gasification experiment adopted a horizontal hole gasification channel. This study combined experimental and theoretical analyses, which is expected to provide a theoretical basis for the field experiment of underground coal gasification. The main objectives of this study are as follow: a) to determine the effect of the different oxygen concentrations on the product gas compositions; b) to determine the effect of the temperature on the product gas compositions; c) to evaluate gasification efficiency using a proposed stoichiometric approach; and d) to estimate gasifier temperature using a proposed heat balance theory.

2.Materials and Methods

2.1 Experimental apparatus

The experiment was carried out in the Energy Research Laboratory of Henan University of Polytechnic. The experimental system of the UCG model comprises the main gasifier body, gasifying agent injection

system, cooling, purification system, and monitoring system. The experimental setup is shown in Figure 2. The main body of the gasifier was made of a steel container, and the external dimension was 2.0 m (length)×1.0 m (width)×1.0 m (height). External walls of the simulated coal seam were covered with refractory cement to prevent heat release and gas leakage. In the lower part of the gasifier at 40 mm from the bottom of the furnace, a horizontal gasification channel was made of hollow steel spring with an inner diameter of 50 mm to prevent the collapse of the coal layer from blocking the gasification channel during the combustion process. The gasifying agent injection system was composed of an air compressor and oxygen generator to provide enough air and oxygen (Pure oxygen) for the experiment. The cooling and purification system was composed of a cooling box and purification box, which are used to cool and filter out impurities such as tar in the gas. A temperature sensor was arranged in the borehole above the coal seam to monitor the temperature of the gasification area in real time. A sampling pump was set in front of the inlet end of the gas chromatograph; this device can effectively pump the gasified gas to the gas chromatograph under the condition of small flow, which can more accurately analyze the gas composition after gasification. The electronic scale under the gasifier monitored the change in the coal seam weight in real time.

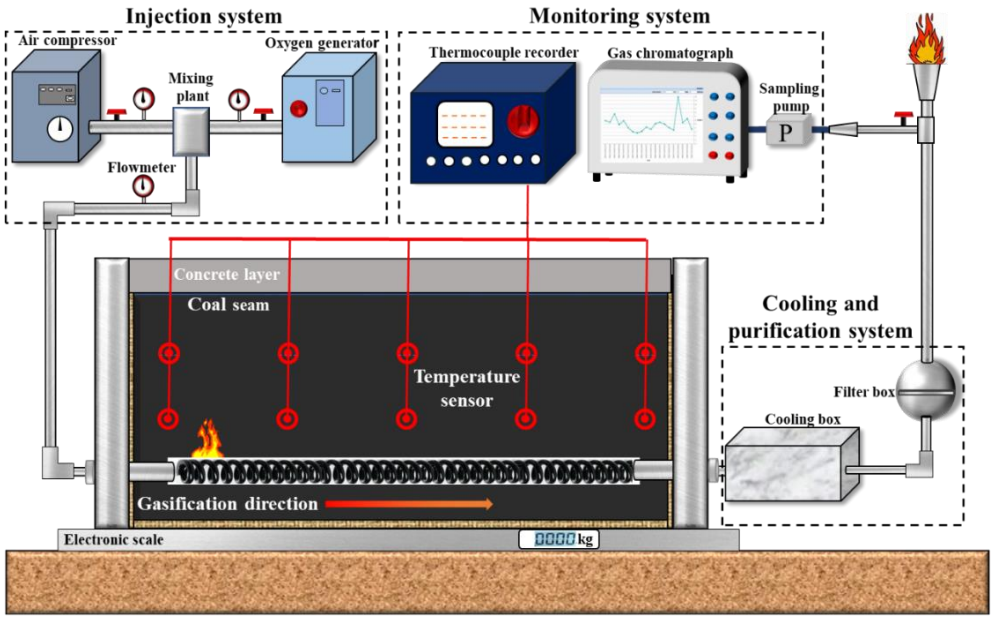

Figure 2. UCG experimental system

2.2 Experimental procedure

2.2.1 Gasification coal sample

In the gasifier, the artificial coal seam was laid layer by layer with coal blocks of length and width of about 100 mm. Additionally, the laying thickness was 400 mm. In the laying process, 100 mm was used as the laying thickness unit 4 times. Each time, the laying plane would be compacted to ensure the structural stability of the artificial coal seam in the gasification process. After the bottom coal seam was laid to 40 mm, the ceramic electric heating ignition plate was embedded. Combustion supporting materials, such as solid alcohol and wood chips, were placed above the ignition disc (Figure 4).

The experimental coal samples were obtained from the Bojianghaizi coal mine in Ordos, Inner Mongolia, China. The results of the proximate analysis and ultimate analysis are shown in Table 1.

Table 1. Proximate and ultimate analysis of coal

No.	Parameter	Value
	Proximate analysis (wt%)	
1	Moisture	3.19
2	Ash	9.2
3	Volatiles	33.06

4	Fixed carbon	54.55
	Ultimate analysis (wt%)	
5	Carbon	79.745
6	Hydrogen	4.42
7	Nitrogen	1.005
8	Oxygen	10.445
9	Sulfur	0.185
10	Calorific value (MJ/kg)	25.74

2.2.2 Gasification agent

Oxygen-enriched air was mainly used as the gasification agent in the experiment. The effects of the oxygen concentration in the gasification agent on the calorific value, temperature, and gasification efficiency were investigated on the premise of other constant test parameters. The injection flow of this gasification experiment is shown in Figure 3. The experiment is carried out in four stages, and the total injection rate of the gasification agent in each stage was constant at 7 m^3/h. The air injection rates of the four stages were 5.3 m^3/h, 4.4 m^3/h, 3.5 m^3/h, and 2.7 m^3/h; the oxygen injection rates were 1.7 m^3/h, 2.6 m^3/h, 3.5 m^3/h, and 4.3 m^3/h; and the oxygen concentrations in the gasification agent were 40%, 50%, 60%, and 70%, respectively.

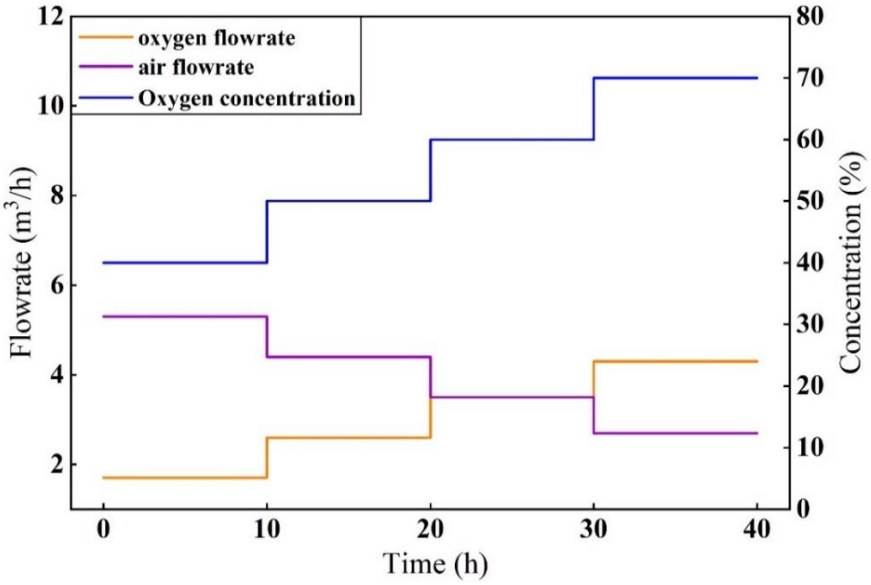

Figure 3. Feed gas flow during the gasification experiments

In the experimental ignition stage, oxygen was introduced into the gasification channel. The igniter was turned on to heat the ignition disk and ignited the combustion supporting materials and nearby coal. The success of the ignition is determined by observing the temperature measured by the thermocouple and the gas composition at the outlet (Figure 4). If the temperature gradually rose to 600℃, the combustible gas components such as H_2, CO and CH_4 continue to rise. The gas generated at the gas production port was successfully ignited, which indicated that the experimental ignition is successful. After the ignition was successful, the gasifying agent was continuously and stably fed in stages according to the preplanned flow, the generated gas was fed into the meteorological chromatograph every 30 minutes to analyze the composition of the produced gas, and the temperature of the gasification chamber and the weight of the gasifier were monitored in real time. At the end of the experiment, N_2 is injected into the gasification area to extinguish the fire.

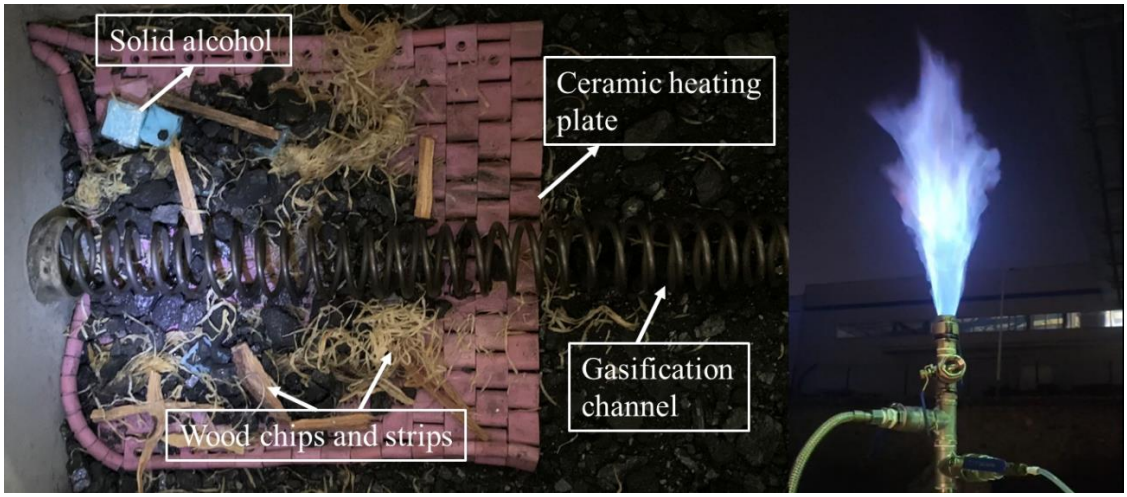

Figure 4. The laid ignition plate and the produced gas that successfully ignited

2.3 Experimental data monitoring

In the UCG process, the temperature distribution in the gasification zone can accurately reflect the experimental gasification process and help investigate the evolution of the gasification zone and the development and evolution of the coal combustion zone. Moreover, the layered temperature monitoring

method was adopted in this experiment. According to the height of the laid artificial coal seam, temperature sensors were installed in the layers with different burial depths so that the temperature distribution characteristics in the different height ranges from the gasification channel can be monitored in real time. The test system was equipped with ten type K thermocouples (Chino Corp) located on both sides of the gasification channel. The sensors T1-1—T1-5 are 60 mm above the gasification channel, the sensors T2-1—T2-5 are 310 mm above the gasification channel, and the interval between the axial sensors is 250 mm. The specific layout position is shown in Figure 5.

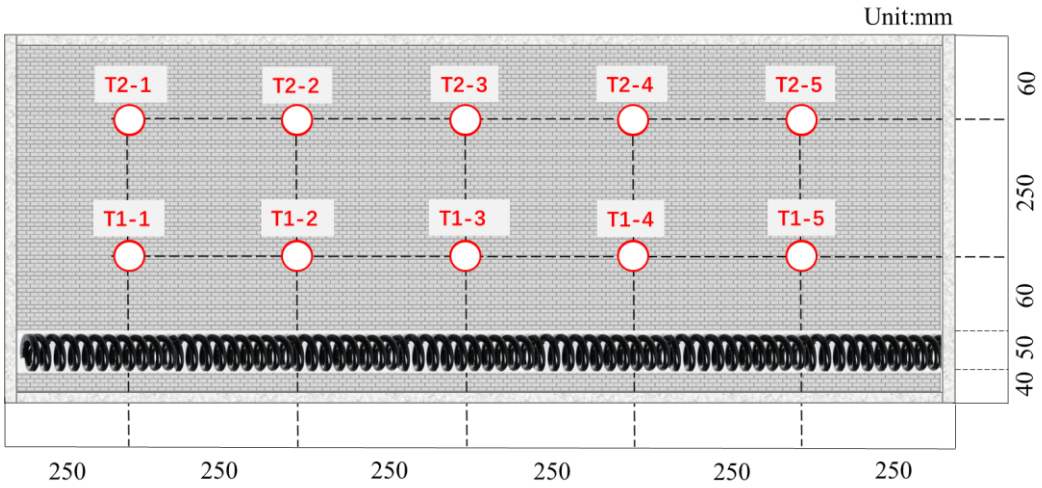

a) Side view

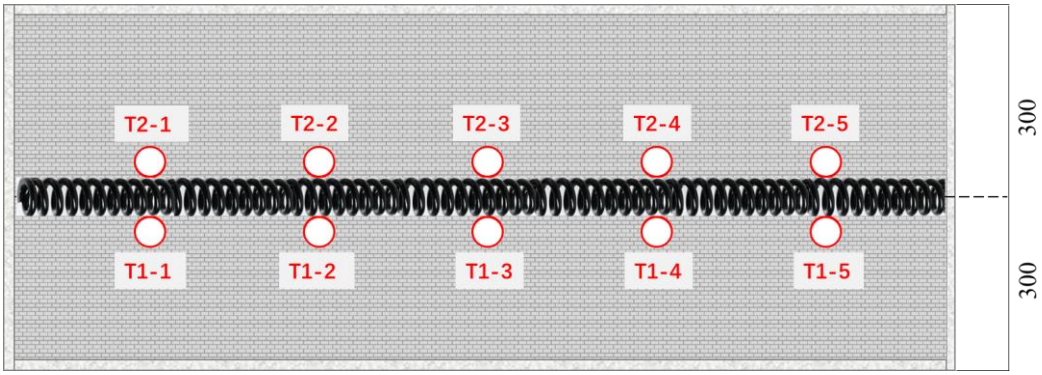

b) Vertical view

Figure 5. Deployment of thermocouples in the experimental reactor

3. Results and Discussion

3.1 Product gas compositions

Figure 6 shows the curves of change in composition and calorific value of the gas produced as a function of reaction time.

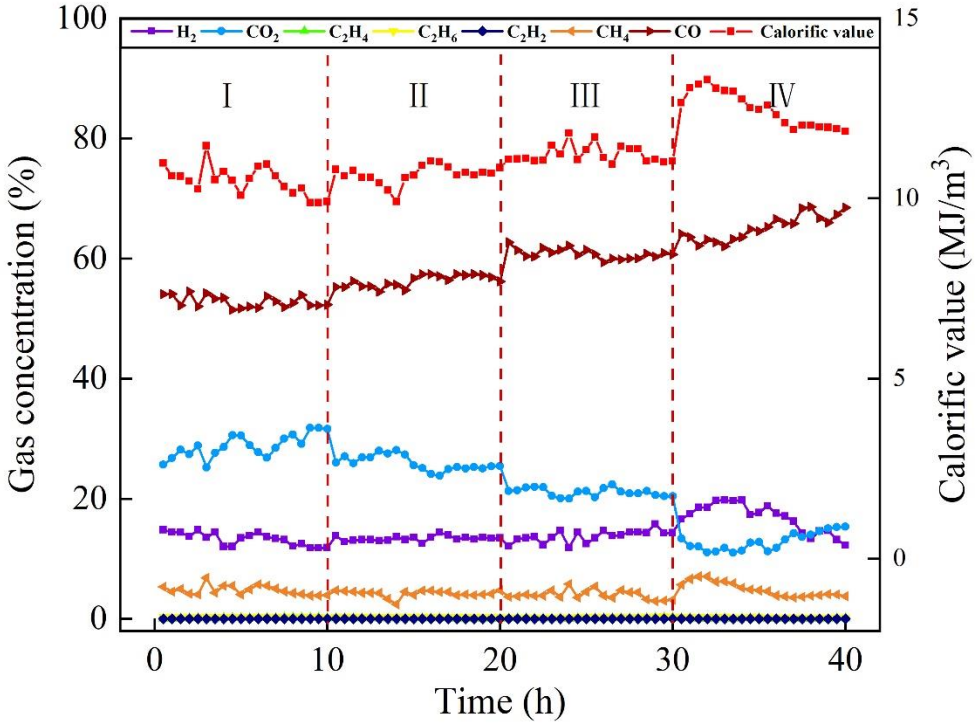

Figure 6. Changes in the calorific value and composition of the gas generated during gasification

By comparing and analyzing the generated gas concentrations in the four stages, the concentration of CO is closely related to the oxygen concentration. Because C+CO=2CO is a strongly endothermic reaction, the reaction equilibrium constant K_P increases sharply when the temperature rises. Thus, the higher the temperature is, the more conducive this temperature increase is to the reaction. With the increase in the oxygen concentration in the experimental model gasifier, the temperature in the gasifier increases. As a result, K_P increases, which is conducive to the reaction and finally increases the content of CO in the gas.

In the first three stages of the experiment, the change in the H_2 and CH_4 content in the generated gas composition was not apparent because the inherent moisture content of the coal sample is only 3.19%,

which is minimal. However, in the early phase of the fourth stage, the concentrations of H_2 and CH_4 significantly increased, possibly because refractory cement was used as the outer wall. During the later stage of the experiment, the combustion expanded to the outer wall. Therefore, the water in the material participated in the gasification process, which increased the H_2 content. H_2 is the primary reactant of the hydrogenation reaction ($C + 2H_2 = CH_4$), and, as a result, the concentration of CH_4 also began to rise. After rising for four hours, the concentrations of H_2 and CH_4 began to decrease, and the water in the outer wall of the cement had been consumed [34].

During the experiment, with the increase of oxygen concentration in the gasification agent, the concentration of the combustible gas in the produced gas and the calorific value of the produced gas show an upward trend. Because the calorific value of the produced gas is calculated according to the concentration of the combustible gas. The changing trend of the calorific value is very close to that of the CH_4 concentration because the heat of combustion of CH_4 is as high as 39.9 MJ/m^3, while the heat of combustion of CO and H_2 is only 12.6 MJ/m^3 and 12.8 MJ/m^3, respectively. Similarly, in the early period of the fourth stage of the experiment, the calorific value showed a significant upward fluctuation, which occurred because the content of CH_4 showed an apparent upward trend. Therefore, even if the proportion of the CH_4 content in the generated gas component is not very large, the influence on the calorific value is still significant.

Table 2. Gasification composition and calorific value

Component volume fraction (%)							Gas calorific value
H_2	CO_2	C_2H_4	C_2H_6	C_2H_2	CH_4	CO	(MJ/m^3)
13.29	28.77	0.11	0.24	0.03	4.75	52.81	10.48
13.35	24.93	0.04	0.24	0.08	4.21	57.15	10.66
13.75	21.04	0.08	0.23	0.02	4.10	60.78	11.26
17.44	12.22	0.02	0.20	0.07	4.92	65.13	12.48

The average concentration and average calorific value of the gas products in each stage are shown in

Table 2. The furnace temperature is low under low oxygen-rich conditions, and CO_2 does not participate effectively in the gasification reaction. Under higher oxygen-rich conditions, the furnace temperature is higher, which facilitates the CO_2 reduction reaction, and the CO content rises. Under the influence of high temperature, due to the release of a large amount of gas, shallow pore coal char is formed in the coal seam cracks, which provides more surface for combustion and gasification reactions [35]. Therefore, increasing the volume fraction of oxygen in the gasification agent can significantly increase the concentration of the combustible gas and improve the calorific value of the underground coal gasification system.

3.2 Temperature monitoring

The temperature field of coal seam and combustion zone affects whether the underground coal gasification can proceed smoothly. The change of temperature in the gasifier is a complex process that is related to a chemical reaction, heat conduction, heat radiation, and heat convection.

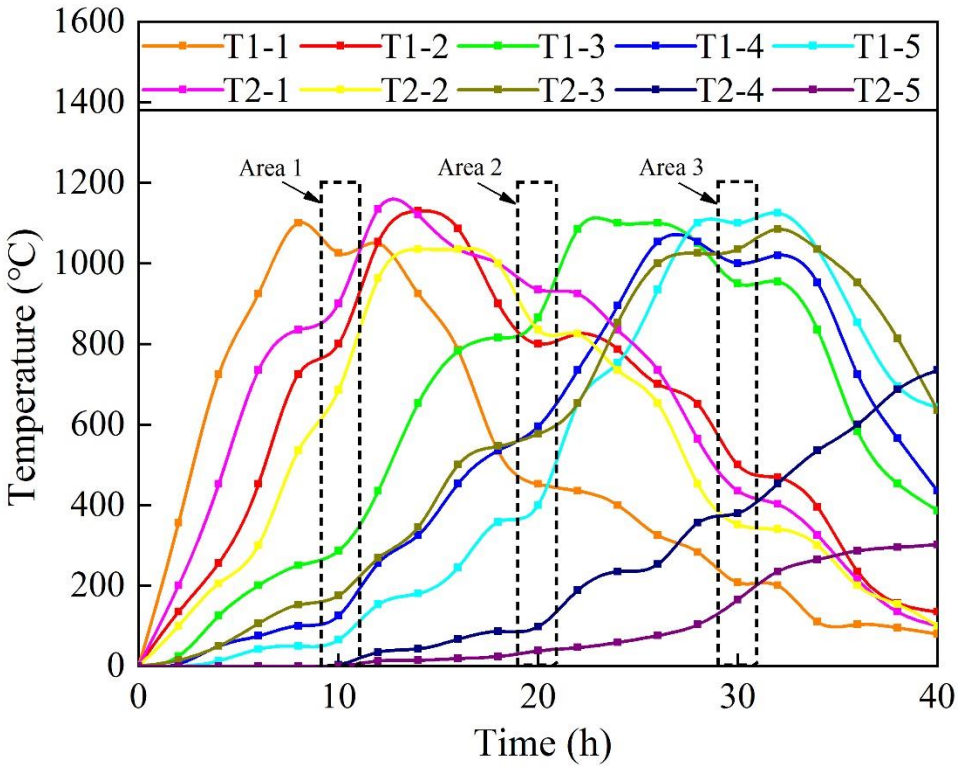

Figure 7. Temperature profiles

Figure 7 shows the curves of the temperature changes with time during the gasification process. The experimental results show that after the successful ignition of the gasifier, the temperature of the gasified coal seam rises sharply, and the influence range dramatically expands. The temperature of T1-1 rises to 1000°C first, which forms a high-temperature gasification chamber centered on the ignition hole. In the first three stages of the experiment, the temperature of the sensor that was located at the top of the gasification channel constantly changed before the temperature of the sensor that was near the gasification channel. The temperature of T2-1 that was above the ignition hole appeared to rise before the temperature of T1-2 that was in front of T2-1. Both temperatures of T2-2 and T2-3 that were in the middle and rear, respectively, appeared to rise before the temperatures of T1-3 and T1-4, which indicated that the temperature field mainly expanded radially along the gasification channel.

These results occurred because, when arranging the coal seam of the gasifier, the plane direction of the coal sample stratification was perpendicular to the gasification channel, and the propagation direction of the coal sample microcarack and crack tends to be parallel to the direction of the stratification plane [36]. The crack in the layer is the primary channel for the inward diffusion of the gasification agent in the initial stage of gasification. The surface with a crack has a larger specific surface area than the surface without a crack. Therefore, this surface can provide more active sites for combustion and gasification reactions. Thus, the combustion and gasification reaction in the coal seam fracture is more substantial than that in the channel.

When the experiment reaches the fourth stage, the temperature of T1-5 changes before the temperatures of T2-4 and T2-5, which indicates that the expansion direction of the coal seam temperature field begins to change. This result occurs because, as the oxygen concentration increases, which causes the coal seam cracking combustion and gasification reactions, excess oxygen begins to diffuse along the

gasification channel, and the surface reactions transpire at the coal walls of the gasification channel.

High-temperature gas diffusion along the channel, heat conduction, heat convection, and heat radiation work together. As a result, the temperature rises faster, which indicates that the temperature field mainly extends in the direction of the gasification channel. Furthermore, from areas 1, 2, and 3, whenever the oxygen concentration in the gasifier rises, the temperature rise rate becomes faster, and the fall rate slows down, which shows that the change in oxygen concentration can affect the trend of the temperature field in the gasifier.

3.3. Energy recovery evaluation

In the UCG process, the degree and rate of reaction are important parameters for efficient gasification, and the accurate calculation of gasification coal consumption is a prerequisite for determining the degree and rate of reaction. However, in practice, gasification coal consumption is not easy to observe and measure on site. Therefore, we propose a method to calculate the coal gasification amount based on carbon balance and provide an energy recovery for judging the gasification efficiency with the help of coal consumption.

3.3.1 Coal consumption of gasification

In the underground gasification process that is based on the conservation of elements in the chemical reaction process, the gasification consumption of coal can be estimated through the gas composition of the generated gas and the known reaction amount of O_2 in the gasification agent. The chemical reactions that occur during the underground gasification of coal can be expressed by the fundamental balance equation, as shown in Equation (1). Based on the results of the elemental analysis of coal, the chemical process can be fully discussed in terms of CH_mO_n, regardless of the specific structure of the coal sample composition.

$$CH_mO_n + \alpha O_2 + \beta H_2O \rightarrow \gamma H_2 + \sigma CO + \varepsilon CO_2 + \eta CH_4 \quad (1)$$

H_2, CO, CO_2 and CH_4 are assumed to be in the dry state, and the denitrogenated oxygen concentrations are p, q, r, and s, respectively. The parameters m and n can be derived from the elemental analysis of coal (m=H/C, n=O/C), where α and β are the equilibrium coefficients of O_2 and H_2O.

The total number of moles of the generated gas is assumed to be equal to Σ.

$$\Sigma = \gamma + \sigma + \varepsilon + \eta \tag{2}$$

The moles γ~η of each gas component are described as follows:

$$\gamma = p\Sigma; \sigma = q\Sigma; \varepsilon = r\Sigma; \eta = s\Sigma \tag{3}$$

$$p + q + r + s = 1 \tag{4}$$

By substituting these values into the carbon balance equation (σ+ε+η=1), the total number of moles Σ can be obtained as:

$$\sum = 1/(q + r + s) \tag{5}$$

Therefore, the following conclusions are drawn:

$$\begin{aligned} \gamma &= \frac{p}{q+r+s}; \sigma = \frac{q}{q+r+s} \\ \varepsilon &= \frac{r}{q+r+s}; \eta = \frac{s}{q+r+s} \end{aligned} \tag{6}$$

The decomposition of water β can be obtained by substituting Equation (6) into the hydrogen equilibrium equation (m+2β=2γ+4η) in Equation (1), as follows:

$$\beta = \frac{p+2s}{q+r+s} - \frac{1}{2m} \tag{7}$$

By substituting Equations (6) and (7) into the oxygen equilibrium equation (n+2α+β=σ+2ε) in Equation (1), the equilibrium coefficient α of O_2 is obtained as follows:

$$\alpha = \frac{q+2r-p-2s}{2(q+r+s)} + \frac{0.5m-n}{2} \tag{8}$$

The coal consumption A (kg/h) is determined by the O_2 consumption (Sm^3/h) and oxygen balance

coefficient α, as shown below:

$$A = \frac{S \times M \times 1.2 \times 1000}{22.4 \times C\% \times \alpha} \quad (9)$$

The term M is the mole fraction of O_2, and C% is the carbon content obtained by industrial analysis.

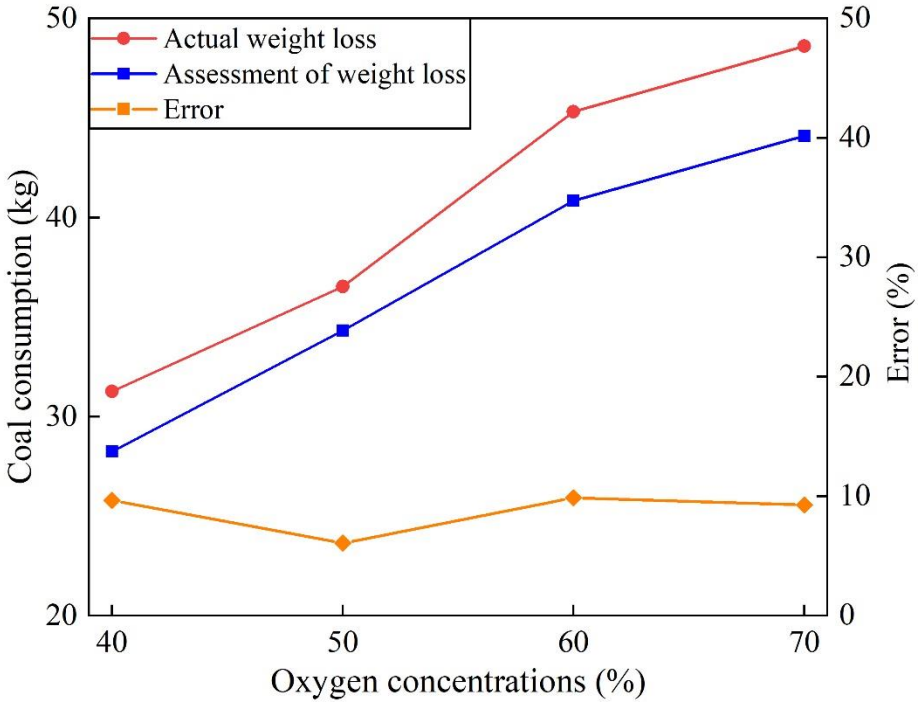

Figure 8. Actual values of model weight loss with estimated values

Figure 8 summarizes the coal consumption that was derived from the average gasification product composition at different gasification stages and the variation in the actual coal weight that was monitored according to the weighing system. Analysis of the data in this figure shows that the coal consumption increases with an increasing oxygen concentration, because as the oxygen concentration increases, the temperature in the gasification chamber increases, and the oxidation reaction in the gasifier occurs more intensely. As a result, more coal is consumed per unit time.

In this experiment, the actual monitored coal consumption was 161.72 kg, while the estimated coal consumption based on the conservation of carbon elements was 147.49 kg. The errors between the measured and estimated values in the four stages were 9.66%, 6.07%, 9.86%, and 9.27%, with an average

of 8.80%. All these error values were less than 10%, which proves that this theory can predict gasification coal consumption. Moreover, the error values may be caused by the evaporation of water from the coal (fissure free water), moisture from incompletely dried concrete, tar filtered by the filtration system, and volatile substances.

Figure 9 shows the actual coal consumption rates for the four stages. As seen from the figure 9, the oxygen concentration increases from 40% to 70%, and the coal consumption rate increases from 2.82 kg/h to 4.41 kg/h, which is an increase of 36.1%. The coal consumption rate can characterize the expansion progress in the combustion chamber; thus, increasing the oxygen concentration can promote the growth rate of the gasification chamber to advance and speed up the reaction process.

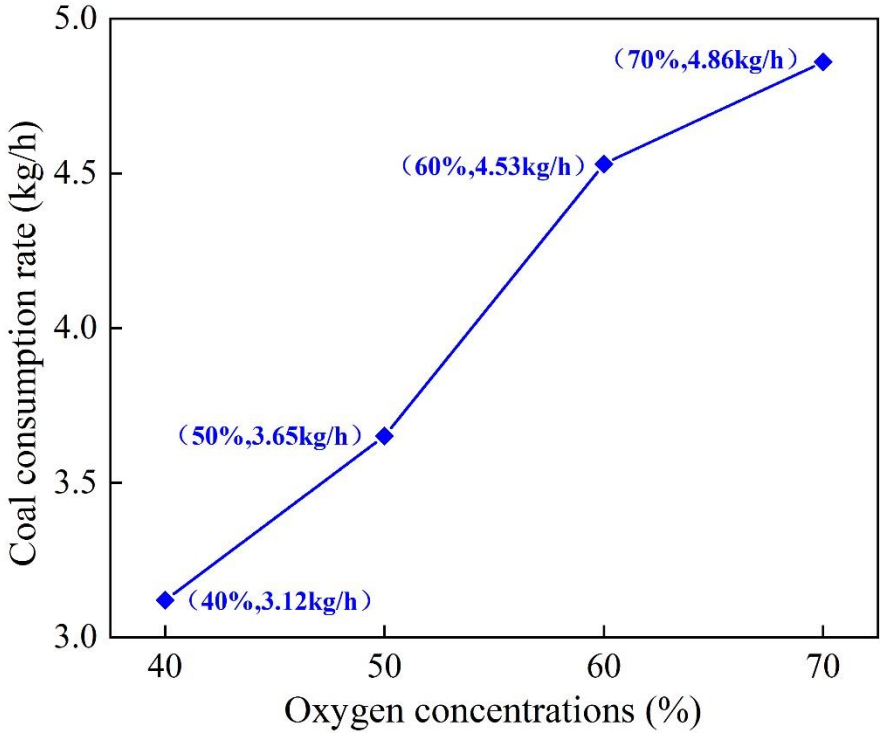

Figure 9. The change in the coal consumption rate at different stages

3.3.2 Energy recovery rate

During the underground gasification of coal, the gasification efficiency is usually judged by the conventional method of comparing the unit calorific value of gasification gas. However, this method

does not provide an accurate description of the efficiency. To further evaluate the gasification efficiency of the experiment, the author presents the definition of the energy recovery ratio (R_g), which is the ratio of the actual gas energy produced to the coal's heat generation. The calculation formula of this ratio is:

$$R_g = \frac{V_d \times \sum_{i=1}^{6} Q_i}{Q_c} \times 100\% \quad (10)$$

Where V_d is the unit gas yield of coal; Q_i is the unit gas calorific value of H_2, CH_4, CO, C_2H_2, C_2H_4, and C_2H_6; and Q_c is the unit calorific value of coal. According to Equation (10), the gasification efficiency of the four stages of this experiment was calculated, as shown in Table 3.

Table 3. Energy recovery rate of the UCG experimental model

Oxygen concentrations (%)	Gas production per unit coal (m^3/kg)	Gas calorific value (MJ/m^3)	Calorific value per unit coal (MJ/kg)	Energy recovery (%)
40	1.71	10.48	25.74	69.63
50	1.76	10.66	25.74	72.89
60	1.77	11.26	25.74	77.43
70	1.73	12.48	25.74	83.88

The experimental results show that the higher the percentage of oxygen in the injection flow is, the higher the gasification efficiency is. When the oxygen concentration increased from 40% to 70%, the energy recovery rate increased from 69.63% to 83.88%, which is an increase of 14.25%. This result implies that the high concentration oxygen injection conditions are beneficial to improving the coal gasification efficiency.

3.4 Temperature assessment modeling

The efficiency of the gasification process is related to the ratio and flow rate of the incoming gasifier and the reaction temperature inside the gasification chamber; although the temperature sensors were arranged in the gasification chamber, the temperature field distribution characteristics of the gasification chamber cannot be accurately obtained due to the limited number of sensors and the complex temperature

variation at each location and stage in the gasification chamber. Therefore, studying a means of estimating the gasification temperature is necessary. The relationship between the heat of reaction and sensible heat in the gasifier is shown in the following equation:

$$H_r = H_{sg} + H_{loss} \quad (11)$$

The reaction heat of gasification (H_r) is equal to the sum of the sensible heat of gas (H_{sg}) and the furnace heat loss (H_{loss}). Because this study added insulated concrete walls around the coal seam, the dissipated heat was ignored. Assuming that the gasifier in this experiment is an adiabatic reactor, the gasification temperature can be predicted based on the gas composition in the furnace.

The reaction equation when the coal is fully reacted is shown below:

$$CH_mO_n + (1 + 0.25m - 0.5n)\,O_2 + \beta H_2O \rightarrow CO_2 + (0.5m + \beta)H_2O \quad (12)$$

The combustion reaction of the gas is shown in the following equation:

$$\gamma H_2 + \sigma CO + \eta CH_4 + (0.5\alpha + 0.5\sigma + 2\eta)O_2 \rightarrow CO_2 + (0.5m + \beta)H_2O \quad (13)$$

According to Equation (1), (12) and (13), the following calculation can be obtained from the heat of reaction (The coefficients of Equations (14-17) can be found in the relevant literature data):

$$Hr = hcoal - (\gamma hH_2 + \sigma hCO + \eta hCH_4) \quad (14)$$

The calorific value of the gas in Equation (14) is shown in Table 4.

Table 4. Heat of combustion of gas

Gas	Value (MJ/m^3)
H_2	12.8
CO	12.6
CH_4	39.9

The sensible heat of the gas is calculated by the following equation:

$$H_{sg} = N \times C_p \times T \quad (15)$$

In this equation, N is the number of moles of the gas, C_P is the specific heat capacity of the gas. The

total sensible heat of each component is determined by comparing the sensible heat of the generated gas H_{sg} and the heat of reaction H_r. When $H_{sg} \neq H_r$, T is reassumed, and the estimation is repeated until $H_{sg}=H_r$; then, the temperature is the gasification temperature. The specific heat capacity of the gas also changes with temperature, and the formula for calculating the specific heat capacity is as follows:

$$Cp = a + bT + cT^2 + dT^3 \quad (16)$$

Table 5 shows the parameters that are used to calculate the specific heat capacity of the gas at different temperature states.

Table 5. Specific heat capacity parameters

Gas composition	a	$b\times10^2$	$c\times10^5$	$d\times10^9$
H_2	6.952	-0.04576	0.09563	-0.2079
CO	6.726	0.04001	0.12830	-0.5307
CO_2	5.316	1.4285	-0.8362	1.7840
CH_4	4.750	1.200	0.303	-2.630
N_2	6.903	-0.03753	0.1930	-0.6861
H_2O	7.700	0.04594	0.2521	-0.8387

Therefore, the sensible heat of each gas component is:

$$Hsg = \int_{25}^{T} (a + bT + cT^2 + dT^3) dT \quad (17)$$

The gas composition monitored at the outlet at a certain moment can be regarded as the average value of the gas composition in the furnace; thus, the calculated gasification temperature is the average gasification temperature in the furnace. Figures 10-13 show the measured (>550°C), estimated and estimated error values of the temperature in the high-temperature gasification region for the four stages of this test.

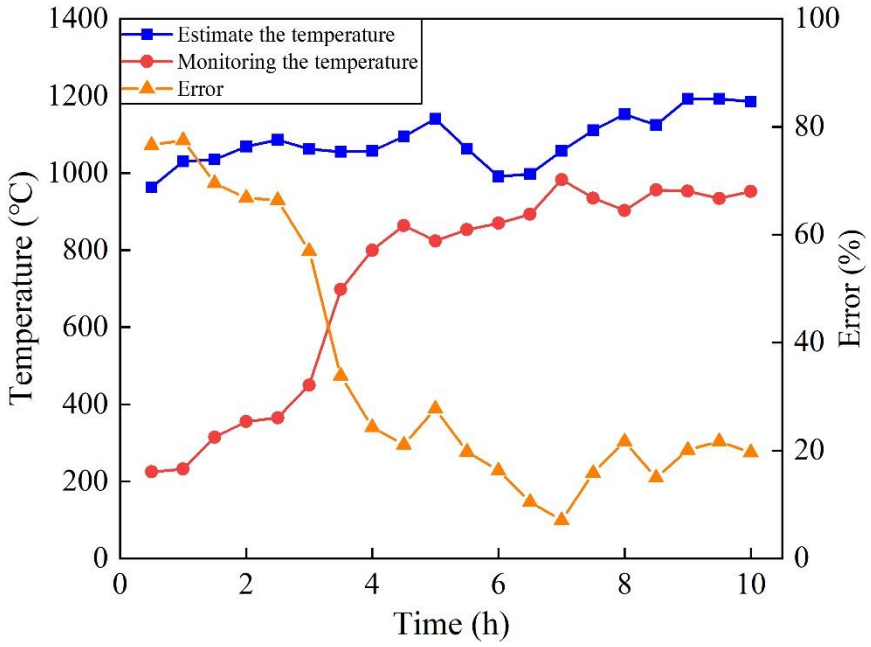

Figure 10. The monitored temperature and estimated temperature change with time

(40% oxygen concentration)

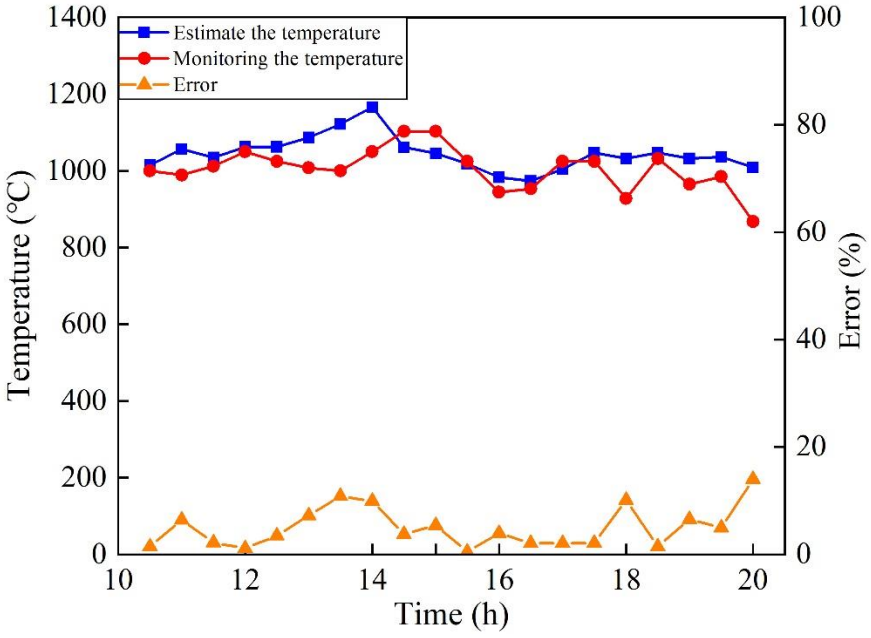

Figure 11. The monitored temperature and estimated temperature change with time

(50% oxygen concentration)

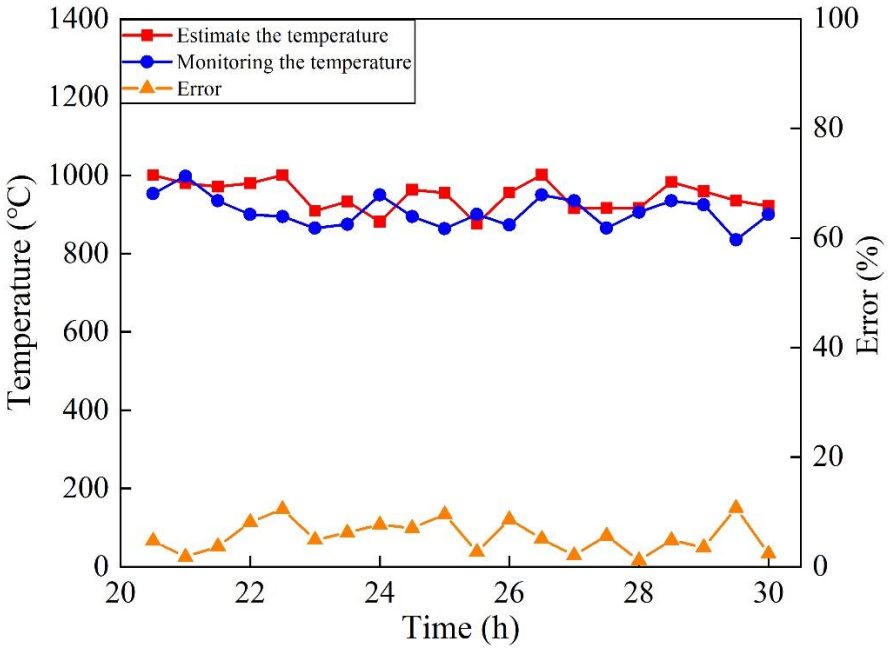

353

354

Figure 12. The monitored temperature and estimated temperature change with time

355

(60% oxygen concentration)

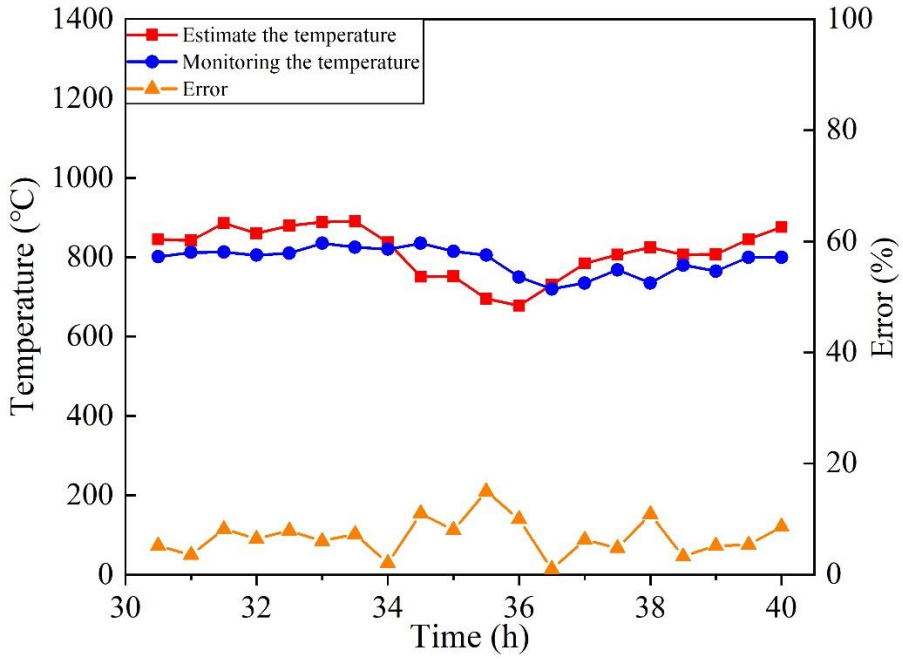

356

357

Figure 13. The monitored temperature and estimated temperature change with time

358

(70% oxygen concentration)

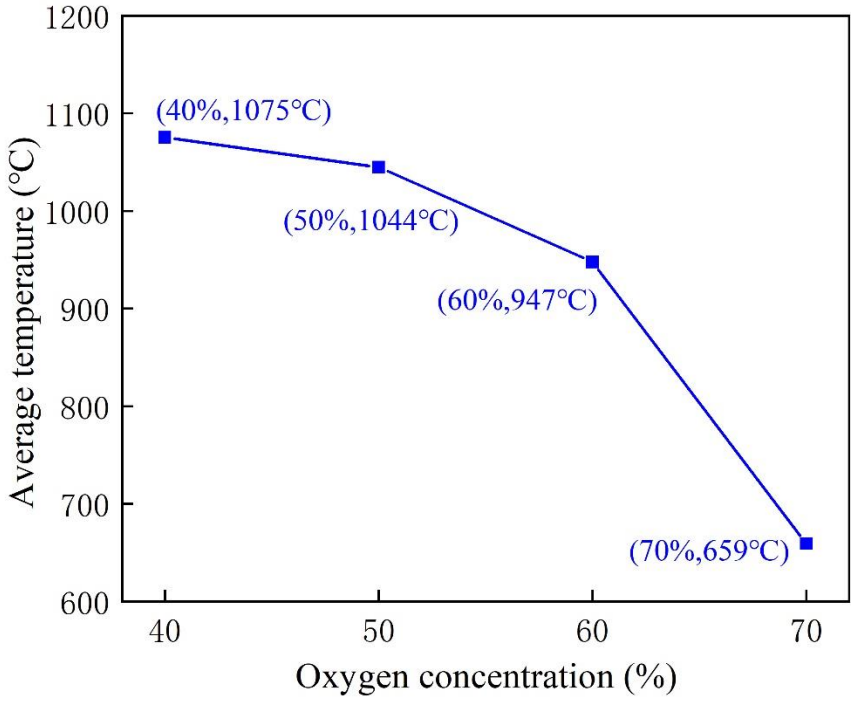

Figure 14. The change in average temperature at different stages

In the beginning of this experiment, the temperature in the furnace was low because the experiment was in the ignition and heating stage. This state was suitable for the dry distillation reaction of coal to proceed. Combustible gases such as CH_4 and H_2 were released from the coal samples around the gasification channel. The calculated temperature was high, so the error between the two kinds was large. After three hours of the experiment, as the temperature of the gasification zone rises, the oxidation and reduction zones began to occupy the main body. The error also began to drop significantly, but still remained at about 20%. This is because the gasification cavity formed at the early stage of gasification is small and the temperature distribution is concentrated and not uniform, so averaging the monitored temperature above 600°C will keep the temperature at a relatively low level; as a result, the error at this stage was large. In the second stage of the experiment, with the gradual expansion of the gasification chamber, the distribution of high-temperature areas became uniform, and the error gradually decreased. The average error in this stage was only 5.32%, while the average errors in the third and fourth stages,

which were both stable at approximately 5%, were 5.56% and 6.80%, respectively. As viewed from all four stages, the estimated temperature was slightly higher than the monitored value overall. This result occurred because the sensible heat value rose due to the lack of the heat loss in the gasifier when calculating the temperature in the gasification section; thus, the estimated temperature was calculated to be on the high side. At some times, such as during the timeframes of 14.5 h-15.5 h in the second stage and 24 h in the third stage, the monitored value was slightly higher than the estimated value. This maybe due to the collapse of the coal seam above the gasification zone, which leads to the increase in the contact face value between the coal sample and the gasification agent. Therefore, the temperature in the gasifier rises rapidly. By calculating the average temperature of the gasification zone (Figure 14), we also found that the gasification temperature showed a downward trend, which indicated that the ratio of the reduction zone to the oxidation zone gradually increased. However, in the fourth stage of the experiment, the gasification temperature was within the temperature range of the reduction zone, between 550 ℃ and 900 ℃, which indicates that the reduction zone occupied the main body of the gasifier. Therefore, we can improve the gasification efficiency by increasing the oxygen concentration. The actual monitored temperatures in the four stages are consistent with the estimated temperature change trend, which proves that this theory can estimate the high-temperature range in the gasification chamber.

Figure 15 shows the relationship between the temperature and heat of reaction for the four stages deduced from this experiment. Fitting the temperature to the heat of reaction data revealed that the heat of reaction was linearly correlated with temperature, and the correlation coefficient was as high as 0.99, which demonstrates this method's reliability.

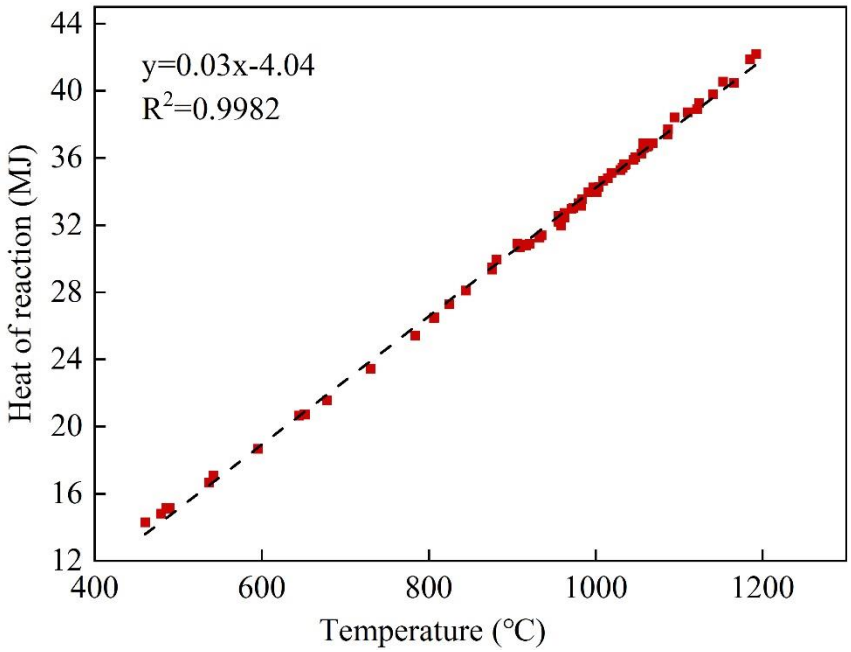

Figure 15. Change of the heat of reaction with temperature

4. Discussion

The gasification agent in this experiment was oxygen-rich air, and no water vapor was added. The H_2 and CH_4 in the gasification products mainly came from the water and hydrogen-containing compounds in the coal samples. The rise in H_2 and CH_4 content in the early part of the fourth stage is probably due to the participation of water in the refractory cement in the gasification reaction. This paper established a theoretical calculation method of coal consumption in the gasification process based on carbon balance. Comparing the actual coal consumption in the test process, the estimated value that is calculated by using this method is 8.7% higher, which may be caused by the evaporation of water from the coal samples as well as from the external concrete, the tar filtered by the filtration system, and the presence of volatile substances. The temperature trend of the whole gasification process can be estimated more accurately based on the heat balance theory. When comparing the estimated value with the monitored value, the estimated value was slightly higher than the monitored value. When estimating the gasification interval temperature, the heat loss in the gasifier was ignored, which increased the estimated sensible heat value.

Therefore, the estimated temperature will rise accordingly. In the later stage, we can add a thermal insulation layer to the gasifier to reduce heat loss and improve the estimation accuracy. However, considering the buried depth of the coal seam in the field experiment, this problem can be solved. In the following study, we will consider the coal seam's dip angle and burial depth to ensure the similarity between the simulation experiment and the field experiment.

5. Conclusion

(1) The volume fraction of oxygen in the gasification agent is one of the main factors that affect the gasification effect. Increasing the oxygen concentration in the gasifier can significantly increase the proportion of combustible gases in the output gas. When the oxygen concentration increased from 40% to 70%, the calorific value of the product gas increased from 10.48 MJ/m^3 to 12.48 MJ/m^3. The experiment conducted demonstrated that the oxygen-enriched air as react gas for sustaining the gasification process is a feasible option.

(2) For UCG field experiments, coal consumption cannot be measured directly. Thus, establishing a model to estimate the coal consumption for UCG experiments is crucial. For this UCG simulation experiment, we compared the theoretically calculated coal consumption with the actual experimental results. The actual value was 161.72 kg and the theoretical estimated value was 147.49 kg. The error percentage was not more than 10%, which indicates that the coal consumption in the gasification process can be estimated by this method.

(3) The evaluation of gas recovery is the reverse deduction of the experimental results from the chemical point of view, so as to evaluate the gasification reaction process. When the volume concentration of injected oxygen increased from 40% to 70%, the energy recovery rate increased from 69.63% to 83.88%. Increasing the volume concentration of the gasifier oxygen can significantly improve

the gasification efficiency of the underground coal gasification system.

(4) Based on the output gas composition, an evaluation model of the underground gasification temperature field of coal was developed by combining the law of thermodynamic conservation. The temperature of the gasification chamber at each stage was evaluated by calculating the reaction heat and sensible heat. After gasification stabilization, the error values of the actual monitored temperature and the theoretical estimated temperature were 5.32%, 5.56% and 6.80%, respectively, which indicates that this theory may be helpful for estimating the temperature of the gasification zone.

Declaration of Competing Interest

The authors declare that they have no known competing financial interests or personal relationships that could have appeared to influence the work reported in this paper.

Acknowledgments: This work was supported by Key Laboratory of Western Mine Exploitation and Hazard Prevention, Ministry of Education (SKLCRKF1902), State Key Laboratory for Geomechanics and Deep Underground Engineering, China University of Mining & Technology (SKLGDUEK2004), Key R & D and promotion projects in Henan Province (16220043), Henan Province Key Scientific Research Project Plan for Colleges and Universities (22B440003).

References

[1] Laciak M, Chen ME. Modeling and control of energy conversion during underground coal gasification process. Energies 2022;15. https://doi.org/10.3390/en15072494.

[2] Qian MG, Jia-Lin XU, Miao XX. Green technique in coal mining. Journal of China University of

Mining & Technology 2003;32(4):344-8. https://doi.org/10.3321/j.issn:1000-1964.2003.04.001.

[3] Bazaluk O, Lozynskyi V, Falshtynskyi V, Saik P, Cabana E. Experimental studies of the effect of design and technological solutions on the intensification of an underground coal gasification process. Energies 2021;14(4):4369. https://doi.org/10.3390/en14144369.

[4] Zhao B, Dong X, Chen Y, Chen S, Chen Z, Peng Y, et al. Experimental investigation on the pore structure evolution of coal in underground coal gasification process 2022. https://doi.org/10.1021/ACSOMEGA.2C00157.

[5] Hu Z, Peng Y, Sun F, Chen S, Zhou Y. Thermodynamic equilibrium simulation on the synthesis gas composition in the context of underground coal gasification. Fuel 2021;293:120462. https://doi.org/10.1016/j.fuel.2021.120462.

[6] Khadse A, Qayyumi M, Mahajani S, Aghalayam P. Underground coal gasification: a new clean coal utilization technique for india. Energy 2007. https://doi.org/10.1016/j.energy.2007.04.012.

[7] Chiesa P, Consonni S, Kreutz T, Williams R. Co-production of hydrogen, electricity and CO_2 from coal with commercially ready technology. Part a: performance and emissions. Int J Hydrogen Energ 2005;30(7):747-67. https://doi.org/10.1016/j.ijhydene.2004.08.002.

[8] Grabowski J, Korczak K, Tokarz A. Aquatic risk assessment based on the results of research on mine waters as a part of a pilot underground coal gasification process. Process Saf Environ 2021;148:548-58. https://doi.org/10.1016/j.psep.2020.10.003.

[9] Pivnyak G, Falshtynskyi V, Dychkovskyi R, Saik P, Koshka O. Conditions of suitability of coal seams for underground coal gasification. Key Engineering Materials 2020;844:38-48. https://doi.org/10.4028/www.scientific.net/KEM.844.38.

[10] Mandal R, Maity T, Chaulya SK, Prasad GM. Laboratory investigation on underground coal gasification technique with real-time analysis. Fuel 2020;275:117865. https://doi.org/10.1016/j.fuel.2020.117865.

[11] Wiatowski M, Kapusta K. Evolution of tar compounds in raw gas from a pilot-scale underground coal gasification (ucg) trial at wieczorek mine in poland. Fuel 2020;276:118070. https://doi.org/10.1016/j.fuel.2020.118070.

[12] Daggupati S, Mandapati RN, Mahajani SM, Ganesh A, Mathur DK, Sharma RK, et al. Laboratory studies on combustion cavity growth in lignite coal blocks in the context of underground coal gasification. Energy 2010;35(6):2374-86. https://doi.org/10.1016/j.energy.2010.02.015.

[13] Selivanova T, V VP, School E. Thermo-chemical conversion of coal samples under high temperature. https://doi.org/10.3969/j.issn.1673-9736.2013.03.03.

[14] Pei P, Nasah J, Solc J, Korom SF, Laudal D, Barse K. Investigation of the feasibility of underground coal gasification in north dakota, united states. Energy Convers Manage 2016;113(Apr.):95-103. https://doi.org/10.1016/j.enconman.2016.01.053.

[15] Vairakannu P, Kumari G. CO_2 enhanced in-situ oxy-coal gasification based carbon-neutral conventional power generating systems. Journal of Energy 2015;84:672-83. https://doi.org/10.1016/j.energy.2015.03.029.

[16] Liu H, Liu S. Exergy analysis in the assessment of hydrogen production from ucg. Int J Hydrogen Energ 2020;45(51):26890-904. https://doi.org/10.1016/j.ijhydene.2020.07.112.

[17] Andrianopoulos E, Korre A, Durucan S. Chemical process modelling of underground coal gasification and evaluation of produced gas quality for end use. Energy Procedia 2015;76:444-

53. https://doi.org/10.1016/j.egypro.2015.07.870.

[18] Zagorak R, Sadasivam S, Thomas HR, Stańczyk K, Kapusta K. Experimental study of underground coal gasification (ucg) of a high-rank coal using atmospheric and high-pressure conditions in an ex-situ reactor. Fuel 2020;270:117490. https://doi.org/10.1016/j.fuel.2020.117490.

[19] Smoliński A, Stańczyk K, Kapusta K, Howaniec N. Chemometric study of the ex situ underground coal gasification wastewater experimental data. Water, Air, & Soil Pollution 2012;223(9):5745-58. https://doi.org/10.1007/s11270-012-1311-5.

[20] Otto C, Kempka T. Synthesis gas composition prediction for underground coal gasification using a thermochemical equilibrium modeling approach. Energies 2020;13. https://doi.org/10.3390/en13051171.

[21] Klebingat S, Kempka T, Schulten M, Azzam R, Fernández-Steeger TM. Optimization of synthesis gas heating values and tar by-product yield in underground coal gasification. Fuel 2018;229:248-61. https://doi.org/10.1016/j.fuel.2018.02.039.

[22] Perkins G, Vairakannu P. Considerations for oxidant and gasifying medium selection in underground coal gasification. Fuel Process Technol 2017;165:145-54. https://doi.org/10.1016/j.fuproc.2017.05.010.

[23] Wang J, Wang Z, Xin L, Xu Z, Gui J, Lu X. Temperature field distribution and parametric study in underground coal gasification stope. Int J Therm Sci 2017;111:66-77. https://doi.org/10.1016/j.ijthermalsci.2016.08.012.

[24] Gur M, Eskin N, Okutan H, Arısoy A, Böke E, Altıntaş Ü, et al. Experimental results of underground coal gasification of turkish lignite in an ex-situ reactor. Fuel 2017;203:997-1006.

https://doi.org/10.1016/j.fuel.2017.03.008.

[25] Massaquoi J, Riggs JB. Mathematical modeling of combustion and gasification of a wet coal slab-I: Model development and verification. Chemical Engineering Science 1983;38(10):1747-56. https://doi.org/10.1016/0009-2509(83)85031-3.

[26] Yang L. The dynamic temperature field of two-stage underground coal gasification (ucg). Energy Sources 2006;28(4/8):667-80. https://doi.org/10.1080/009083190951438.

[27] Xi J, Liang J, Sheng X, Shi L, Li S. Characteristics of lump lignite pyrolysis and the influence of temperature on lignite swelling in underground coal gasification. J Anal Appl Pyrol 2016;117(Jan.). https://doi.org/10.1016/j.jaap.2015.11.011.

[28] Yang D, Sarhosis V, Sheng Y. Thermal–mechanical modelling around the cavities of underground coal gasification. J Energy Inst 2014;87(4):321-9. https://doi.org/10.1016/j.joei.2014.03.029.

[29] Prabu V, Jayanti S. Heat-affected zone analysis of high ash coals during ex situ experimental simulation of underground coal gasification. Fuel 2014;123:167-74. https://doi.org/10.1016/j.fuel.2014.01.035.

[30] Kapusta K, Stańczyk K, Wiatowski M, Chećko J. Environmental aspects of a field-scale underground coal gasification trial in a shallow coal seam at the experimental mine barbara in poland. Fuel 2013;113:196-208. https://doi.org/10.1016/j.fuel.2013.05.015.

[31] Liu HT, Yao H, Yao K, Chen F, Luo GQ. Characteristics of "three zones" during underground coal gasification. Advanced Materials Research 2012;524-527:56-62. https://doi.org/10.4028/www.scientific.net/AMR.524-527.56.

[32] Liu H, Feng C, Xia P, Kai Y, Liu S. Method of oxygen-enriched two-stage underground coal

gasification. Mining Science and Technology (China) 2011;21(2):191-6. https://doi.org/10.1016/j.mstc.2011.02.018.

[33] Wang Z, Huang W, Zhang P, Xin L. A contrast study on different gasifying agents of underground coal gasification at huating coal mine. Journal of Coal Science and Engineering (China) 2011;17(2):181-6. https://doi.org/10.1007/s12404-011-0214-1.

[34] Hamanaka A, Su F, Itakura K, Takahashi K, Kodama J, Deguchi G. Experimental study on evaluation of underground coal gasification with a horizontal hole using two different coals. Fuel 2021;305:121556. https://doi.org/10.1016/j.fuel.2021.121556.

[35] Wang Z, Wei Y, Hou T, Jin Y, Wang C, Liang J. Large-scale laboratory study on the evolution law of temperature fields in the context of underground coal gasification. https://doi.org/10.1016/j.cjche.2020.07.005.

[36] Su FQ, Itakura KI, Deguchi G, Ohga K. Monitoring of coal fracturing in underground coal gasification by acoustic emission techniques. Appl Energ 2017;189(MAR.1):142-56. https://doi.org/10.1016/j.apenergy.2016.11.082.

Declaration of interests

☒ The authors declare that they have no known competing financial interests or personal relationships that could have appeared to influence the work reported in this paper.

☐The authors declare the following financial interests/personal relationships which may be considered as potential competing interests:

Credit Author Statement

Fa-qiang Su.: Investigation, Writing-Reviewing and Editing, Funding acquisition.

Tao-Zhang: Investigation, Writing-Original draft preparation, Funding acquisition.

Jun-bo Wu: Supervision, Validation.

Qi-chao Deng: Investigation, Data curation.

Akihiro Hamanaka: Conceptualization, Methodology.

Yi-he Yu: Investigation, Validation, Data curation, Funding acquisition.

Jun-nan Yang: Validation, Resources.

Meng-jia Dai: Investigation, Validation.

Xiao-long He: Investigation , Data curation.